4 Infrared Imaging

William Danchi, NASA Goddard Space Flight Center, Chair

Peter Lawson, Jet Propulsion Laboratory, Co-Chair

Olivier Absil, Rachel Akeson, John Bally, Richard K. Barry, Charles Beichman, Adrian Belu, Mathew Boyce, James Breckinridge, Adam Burrows, Christine Chen, David Cole, David Crisp, Rolf Danner, Peter Deroo, Vincent Coudé du Foresto, Denis Defrère, Dennis Ebbets, Paul Falkowski, Robert Gappinger, Ismail D. Haugabook, Sr., Charles Hanot, Thomas Henning, Phil Hinz, Jan Hollis, Sarah Hunyadi, David Hyland, Kenneth J. Johnston, Lisa Kaltenegger, James Kasting, Matt Kenworthy, Alexander Ksendzov, Benjamin Lane, Gregory Laughlin, Oliver Lay, Réne Liseau, Bruno Lopez, Rafael Millan-Gabet, Stefan Martin, Dimitri Mawet, Bertrand Mennesson, John Monnier, Naoshi Murakami, M. Charles Noecker, Jun Nishikawa, Meyer Pesesen, Robert Peters, Alice Quillen, Sam Ragland, Stephen Rinehart, Huub Rottgering, Daniel Scharf, Eugene Serabyn, Motohide Tamura, Mohammed Tehrani, Wesley A. Traub, Stephen Unwin, David Wilner, Julien Woillez, Neville Woolf, and Ming Zhao

4.1 Introduction

This chapter describes the science and technology of infrared and mid-infrared missions capable of detecting and characterizing exoplanets through the interferometric nulling of starlight.

A probe-scale mission of this type would image nearby planetary systems, and allow us to study planet formation, study structure in debris and exozodiacal disks, and detect and characterize warm Jupiters, and possibly Super-Earths. Planets around ~50 stars would be characterized. A probe-scale mission would provide transformative science and would lay the engineering groundwork for the flagship mission that would follow.

A flagship mission would enable the detection of biosignatures in the spectra of Earth-like planets of 200 or more nearby target stars. Such a mission would have the highest angular resolution for planet-finding of any of the mission concepts described in this Report.

The missions described in this chapter have grown from the legacy of the Terrestrial Planet Finder (TPF), which with its counterpart in Europe, the Darwin mission, have been studied and reviewed since the mid-1990s. Technology development for TPF was endorsed by the McKee-Taylor report (National Research Council 2001) with the goal of enabling a mission sometime after 2010. Here we report on the success of that investment.

As will be shown in this chapter, the technology for a probe-scale mission is largely in hand. A probe-scale mission would use a fixed or connected-structure and operate at infrared wavelengths. Laboratory experiments in starlight suppression have already exceeded flight requirements for such a mission by a factor of 10, and all of the necessary component

hardware has been demonstrated in the lab. Future technology efforts should include some additional system-level testing and modeling, and cryogenic demonstration of single-mode fibers. The probe-scale mission that is presented is the Fourier Kelvin Stellar Interferometer (FKSI), as described by Danchi et al. (2003).

Further sustained effort is nonetheless required to address several of the risks associated with a flagship mission. The major risk of such a mission is dominated by the reliance on a simultaneous and coordinated use of five spacecraft flying in formation; four telescopes each on separate spacecraft and an additional spacecraft for a beam combiner. Guidance, navigation, and control demonstrations have shown that such control is feasible, but actual hardware tests in space have not yet been performed. On the other hand, interferometric nulling has now reached the performance level required for flight, as demonstrated through the Adaptive Nuller testbed. Future technology development should include cryogenic system-level tests with mature brassboard designs and space-based demonstrations of formation flying maneuvers using representative sensors and thrusters. The flagship mission that is presented is the Terrestrial Planet Finder Interferometer (TPF-I), identical to the Darwin mission concept that was proposed to the European Space Agency's Cosmic Vision program in 2007.

Although we support most of the long-term goals that the Exoplanet Task Force (ExoPTF) recommended for a flagship infrared mission, we recommend a different path forward for the near-term. Specifically, we are not convinced, as the ExoPTF report suggests, that the problem of exozodi levels and debris disks can be solved with ground-based observations to the extent necessary for the formulation of a flagship mission. We are not convinced, in part due to our own experience with the Keck Interferometer, for which the lower limit on exozodis is 100–200 times that of the Solar System zodi level. We expect that the nulling instrument on Large Binocular Telescope Interferometer (LBTI) will reduce this limit substantially for a relatively small sample of stars. We discuss how a probe-class mission in the infrared can measure the exozodi levels down to the level of one Solar System zodi for essentially *all* of the potential target stars for the eventual flagship TPF/Darwin missions. This step is crucial, not only for the flagship characterization missions, but is also of great value to an astrometric mission because that mission can then focus its searches for Earth-twins around stars with low exozodi levels. Moreover, an infrared probe-class mission has a higher degree of technology leveraging from *JWST*, and could be undertaken in a relatively short time without undue cost and technology risk. Our summary of recommendations from this chapter follows:

Recommendation: A vigorous technology program, including component development, integrated testbeds, and end-to-end modeling, should be carried out in the areas of formation flying and mid-infrared nulling, with the goal of enabling a probe-scale nulling interferometry mission in the next 2 to 5 years and a flagship mission within the next 10 to 15 years.

Recommendation: The fruitful collaboration with European groups on mission concepts and relevant technology should be continued.

Recommendation: R&A should be supported for the development of preliminary science and mission designs. Ongoing efforts to characterize the typical level of exozodiacal light around Sun-like stars with ground-based nulling interferometry should be continued.

In this chapter, we outline the scientific parameter space afforded by the next generation of mid-infrared interferometers in the context of ground-based arrays, including the Atacama Large Millimeter Array (ALMA), the Keck Interferometer (KI), the Large Binocular

Telescope Interferometer (LBTI), and the Very Large Telescope Interferometer (VLTI), as well as cooled space telescopes (*Spitzer, Herschel*, *JWST*).

The remainder of this chapter is divided into self-contained sections on Science Goals (§4.1), Observatory Concepts (§4.2), Technology (§4.3), and Research & Analysis Goals (§4.4).

4.1.1 Sensitivity and Angular Resolution

Both high-angular resolution and high sensitivity in the mid-infrared are key to future progress across all major fields of astronomy. Figure 4-1 shows the parameter space of spatial resolution versus sensitivity, illustrating the trade-offs between the high sensitivity possible in space and the high angular resolution achievable from the ground. This diagram highlights the rich and varied science goals made possible by continued incremental technical developments for advanced imaging in the mid-infrared.

Processes occurring at 0.5–5 AU in protoplanetary disks enable the formation of giant and terrestrial planets and are revealed by observations in the mid-infrared, which are sensitive to dust emission from 100–1000 K.

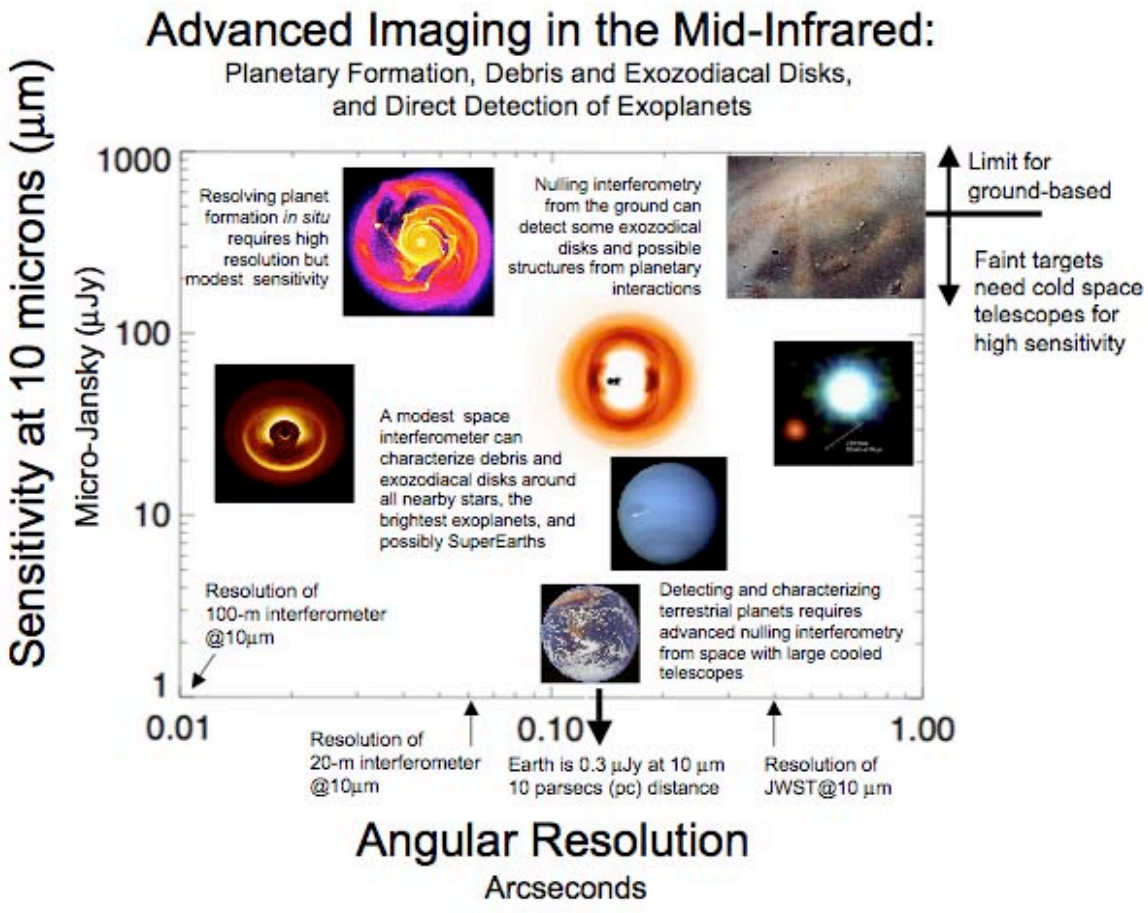

Figure 4-1. Relationship between resolution and sensitivity as it pertains to advanced imaging in the infrared for planet formation, debris and exozodial disks, and direct detection of exoplanets. (W. C. Danchi, NASA GSFC)

Achieving the necessary angular resolution at infrared and mid-infrared wavelengths to study protoplanetary disks requires long-baseline interferometry with ~100–250-m baselines to probe 1-AU scales for the nearest star-forming regions at a distance of 140 pc. Such baselines are already possible from the ground. The KI and the VLTI are now able to probe the dust and temperature structure around luminous Herbig Ae stars and T Tauri disks. The study of planet formation is being revolutionized by mid-IR interferometry's sensitivity to the warm inner disk and soon will be augmented by ALMA's probe of the cold outer disk. Although the next-generation millimeter-wave interferometer ALMA will lack the angular resolution to probe the terrestrial planet formation zone, mid-infrared interferometry with > 250 meter baselines will be sensitive to warm dust emission within the inner few AUs of planet-forming disks.

However, thermal emission from the atmosphere and telescope limits the sensitivity of ground-based observations, driving most science programs towards space platforms. Even very modest sized cooled apertures can have orders of magnitude more sensitivity in the thermal infrared than the largest ground-based telescopes currently planned or in operation.

4.1.2 Probe-Scale Mission Science Goals

Advanced Imaging in the Mid-infrared: Planet Formation, Debris and Exozodiacal Disks, Warm Jupiters, and Super-Earths

The more modest baselines of ~10–20 m, attainable with a probe-scale mission, would be capable of measuring solar-system features around nearby stars.

A probe-scale mission would focus on three main science goals for further study of greatest importance to the direct detection of exoplanets in the infrared, namely (1) measure resonant structures in exozodiacal disks, their flux levels, and the chemical evolution of the material they contain, (2) detect and characterize the atmospheres of nearby exoplanets, including those currently known and those that may be discovered by this technique, and (3) survey prospective target stars for levels of exozodical dust.

Measure Resonant Structures in Exozodiacal Disks

The optically-thick and gas-rich disks out of which planets form are bright, dominating over the emission from the central star. As the system evolves, the dust grains grow into progressively larger bodies, and the gas dissipates. Small particles of dust still pervade the system, created in collisions between planetesimals, and occasionally large collisions will produce dramatic structure in these "debris disks." Here, mid-infrared imaging in conjunction with nulling (to block out the central star), allows the spatial distribution and spectral energy distribution (SED) of the debris disks to be scrutinized. Ground- and space-based interferometers both have important roles here, since ground systems can probe brighter debris disks with greater angular resolution (necessary to null out the star without nulling out the dust) and the space systems with modest ~20-m baseline can sensitively look for debris around nearby stars.

Exozodiacal disks are already under intensive study because the mid-IR emission and scattered light can mimic or hide the signal of terrestrial planets around nearby stars. Chapter 5 is devoted to this crucial topic, and we refer the reader to that chapter for further details.

Detect and Characterize Nearby Exoplanets

Planned mid-infrared facilities are also being designed to directly detect exoplanets using nulling interferometry. Ground-based systems can contribute at shorter wavelengths (< 5 μm) but exoplanet detection in the mid-infrared (6–20 μm) is not expected to be practical from the ground because thermal emission from the warm sky and telescope swamps the faint planetary signal (except perhaps in some rare scenarios). A probe-scale mission could be used to characterize the atmospheres of a large number of the currently known massive exoplanets and possibly Super Earths (e.g., Danchi et al. 2003a,b), whereas a flagship formation-flying interferometer could also detect terrestrial planets and search for atmospheric biomarkers.

Characterize the Atmospheric Constituents of Giant Planets

A probe-scale mission would have sufficient sensitivity to detect and characterize a broad range of exoplanets. Many molecular species, such as carbon monoxide, methane, and water vapor, have strong spectral features in the 3–8 μm region, as can be seen in Figure 4-2, which displays model atmospheres for planets at various distances from the host star, for exoplanets as calculated by Seager et al. (2005). The red curve shows the theoretical spectrum of a very hot, close-in planet at 0.05 AU, and the blue curve displays the spectrum for a much cooler planet ten times further out, at 0.5 AU. Also displayed are sensitivity curves for the IRAC instrument on *Spitzer* (light blue) and the curve for a representative probe-scale mission, FKSI (purple).

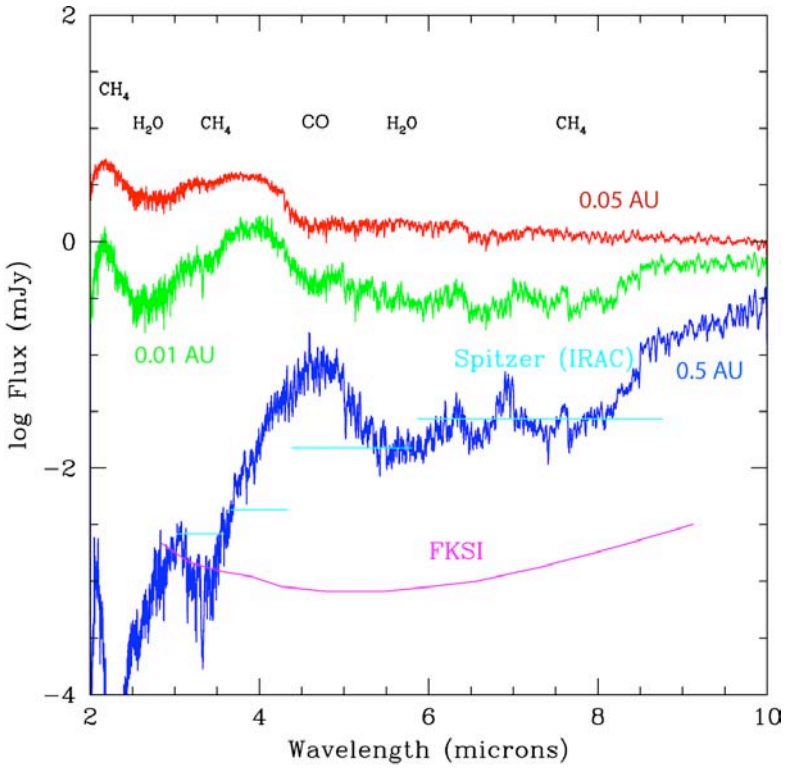

Figure 4-2. The FKSI system can measure the spectra of exoplanets with a wide range of semi-major axes.

Characterize the Atmospheres of Super Earths

The apparently commonplace nature of lower mass planets suggests an intermediate class of planets, Super Earths, may be observable with a probe-scale mission. A prime example of this is the planetary system of GL 581. The outer two planets of this system are near the habitable zone of the star. Selsis et al. (2007) have analyzed this system and suggest the outer planet (planet d, a = 0.25 AU, $R \sim 2R_{\oplus}$, $M \sim 8\ M_{\oplus}$) is the most likely to be habitable. Since the star is at 6.3 pc, the planet's angular separation, 0.04 arcsec, is at the first maximum of the fringe pattern of FKSI. At four times the flux of an Earth-size planet, GL 581d would be within the sensitivity limit of FKSI. Thus, there is already one known, possibly Earth-size planet that could be observed with FKSI. As more Super Earths are discovered, it is likely that FKSI will have at least a small sample of objects that might be characterized for the atmospheric constituents and could indicate habitability.

Characterize the Dynamical Environment of the Habitable Zone

In addition to observations of the atmospheres of giant planets, a probe-scale mission can contribute to our understanding the typical distribution of giant planets in wide orbits (> 5-10 AU). Such planets can dominate the dynamical environment of the habitable zone, and affect the delivery of volatiles to terrestrial planets (Lunine 2001). Planets on eccentric orbits may disrupt the habitable zone or affect the composition by perturbation of outer planetesimals into crossing orbits with the habitable zone. Understanding the placement and orbital parameters of outer planets is an important prerequisite to searching for terrestrial planets in these systems. Such observations are difficult to obtain from ground-based telescopes. Massive or young planets can be detected (cf. Lafrenière et al. 2008; Hinz et al. 2006), but planets that are older than ~0.5 Gyr or are less massive than Jupiter are not detectable with 8-m class ground-based telescopes.

Survey the Exozodiacal Dust of Target Stars

Knowing which nearby main-sequence stars have the lowest amount of zodiacal dust will allow for a more efficient strategy of spectral characterization of Earth-sized planets. This information could also be used to optimize the search strategy for an astrometric mission. A probe-scale infrared mission would enable an exozodiacal dust survey (< 1 zodi at < 1 to > 4 AU) including infrared spectra to elucidate grain chemistry and evolution, disk structure, and brightness, for all the likely target stars of a flagship mission within 30 pc of the Solar System.

4.1.3 Flagship Mission Science Goals and Requirements

Search for Habitability and Signs of Life

A flagship mission would be designed to detect terrestrial exoplanets around nearby stars and measure their spectra (e.g., Beichman et al. 1999, 2006; Fridlund 2000; Kaltenegger & Fridlund 2005). These spectra would be analyzed to establish the presence and composition of the planets' atmospheres, to investigate their capability to sustain life as we know it (habitability), and to search for signs of life. A flagship mission would also have the capacity to investigate the physical properties and composition of a broader diversity of planets, to understand the formation of planets, and to search for the presence of potential biosignature compounds. The range of characteristics of planets is likely to exceed our experience with the planets and satellites in our own Solar System. Moreover, Earth-like

planets orbiting stars of different spectral type may also be expected to evolve differently (Selsis 2000; Segura et al. 2003, 2005).

Biomarkers are detectable species whose presence at significant abundance requires a biological origin (Des Marais et al. 2002). They are the chemical ingredients necessary for biosynthesis (e.g., oxygen [O_2] and CH_4) or are products of biosynthesis (e.g., complex organic molecules, but also O_2 and CH_4). Our search for signs of life is based on the assumption that extraterrestrial life shares fundamental characteristics with life on Earth, in that it requires liquid water as a solvent and has a carbon-based chemistry (Owen 1980; Des Marais et al. 2002). Therefore, we assume that extraterrestrial life is similar to life on Earth in its use of the same input and output gases, that it exists out of thermodynamic equilibrium, and that it has analogs to bacteria, plants, and animals on Earth (Lovelock 1975). Figure 4-3 displays the observed emission spectrum from the Earth in the infrared.

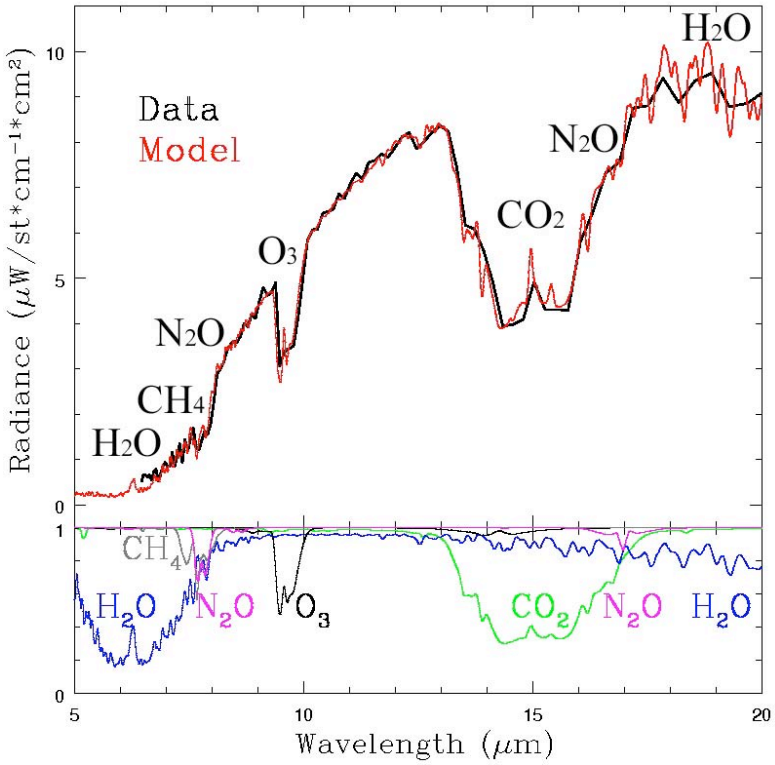

Figure 4-3. Observed emission spectrum in the infrared (Christensen & Pearl 1997) of the integrated Earth, as determined from Earthshine and space respectively. The data is shown in black, model and individual chemical feature color. (Kaltenegger, Traub & Jucks 2007)

Candidate biomarkers that might be detected by a flagship mission with a low-resolution instrument include O_2, O_3, and CH_4. There are good biogeochemical and thermodynamic reasons for believing that these gases should be ubiquitous byproducts of carbon-based biochemistry, even if the details of alien biochemistry are significantly different than the biochemistry on Earth. Production of O_2 by photosynthesis allows terrestrial plants and photosynthetic bacteria (cyanobacteria) to use abundant H_2O as the electron donor to reduce CO_2, instead of having to rely on scarce supplies of hydrogen (H_2) and hydrogen sulfide (H_2S). Oxygen and nitrous oxide (N_2O) are two very promising bio-indicators. Oxygen is a chemically reactive gas. Reduced gases and oxygen have to be produced concurrently to produce quantities large enough to be detectable in disk-averaged spectra

of terrestrial planet atmospheres, as they react rapidly with each other. N_2O is a biomarker in the Earth's atmosphere, being produced in abundance by life but only in trace amounts by natural processes. Although a relatively weak feature in the Earth's spectrum, it may be more pronounced in terrestrial exoplanet atmospheres of different composition or host-star spectral type (Segura et al. 2005). Currently, efforts are ongoing to explore the plausible range of habitable planets and to improve our understanding of the detectable ways in which life modifies a planet on a global scale.

In the mid-IR, the classical signature of biological activity is the combined detection of the 9.6-μm O_3 band, the 15-μm CO_2 band, and the 6.3-μm H_2O band or its rotational band that extends from 12 μm out into the microwave region (Selsis & Despois 2002). The oxygen and ozone absorption features in the visible and thermal infrared, respectively, could indicate the presence of photosynthetic biological activity on Earth any time during the past 50% of the age of the Solar System. In the Earth's atmosphere, the 9.6-μm O_3 band is a poor quantitative indicator of the O_2 amount, but an excellent qualitative indicator for the existence of even traces of O_2. The O_3 9.6-μm band is a very nonlinear indicator of O_2 for two reasons. First, for the present atmosphere, low-resolution spectra of this band show little change with the O_3 abundance because it is strongly saturated. Second, the apparent depth of this band remains nearly constant as O_2 increases from 0.01 times the present atmosphere level (PAL) of O_2 to 1 PAL (Segura et al. 2003). The primary reason for this is that the stratospheric ozone increases that accompanied the O_2 buildup lead to additional ultraviolet heating of the stratosphere. At these higher temperatures, the stratospheric emission from this band partially masks the absorption of upwelling thermal radiation from the surface.

Methane is not readily identified using low-resolution spectroscopy for present-day Earth, but the CH_4 feature at 7.66 μm in the IR is easily detectable at higher abundances (Kalteneggar, Traub & Jucks 2007). When observed together with molecular oxygen, abundant CH_4 can indicate biological processes (see also Lovelock 1975; Segura et al. 2003). Depending on the degree of oxidation of a planet's crust and upper mantle, non-biological mechanisms can also produce large amounts of CH_4 under certain circumstances.

N_2O is also a candidate biomarker because it is produced in abundance by life but only in trace amounts by natural processes. There are no N_2O features in the visible and three weak N_2O features in the thermal infrared at 7.75 μm, 8.52 μm, and 16.89 μm. For present-day Earth, one needs a resolution of 23, 23 and 44, respectively, to detect these N_2O features at thermal infrared wavelengths (Kaltenegger, Traub & Jucks 2007). Spectral features of N_2O also become more apparent in atmospheres with less H_2O vapor. Methane and nitrous oxide have features nearly overlapping in the 7-μm region, and additionally both lie in the red wing of the 6-μm water band. Thus, N_2O is unlikely to become a prime target for the first generation of space-based missions searching for exoplanets, but it is an excellent target for follow-up missions. There are other molecules that could, under some circumstances, act as excellent biomarkers, e.g., the manufactured chloro-fluorocarbons (CCl_2F_2 [Freon 13] and CCL_3F [Freon 12]) in our current atmosphere in the thermal infrared waveband, but their abundances are too low to be spectroscopically observed at low resolution.

Other biogenic trace gases might also produce detectable biosignatures. Currently identified potential candidates include volatile methylated compounds (like methyl chloride [CH_3Cl]) and sulfur compounds. It is known that these compounds are produced by microbes, and preliminary estimates of their lifetimes and detectability in Earth-like atmospheres around stars of different spectral type have been made (Segura et al. 2003, 2005). However, it is not yet fully understood how stable (or detectable) these compounds would be in

atmospheres of different composition and for stars of different spectral type and incident ultraviolet flux. These uncertainties, however, could be addressed by further modeling studies.

Science Requirements

The requirement for a flagship-class mission to detect directly and characterize Earth-like planets around nearby stars implies that the mission must determine the type of a planet and characterize its gross physical properties and its main atmospheric constituents, thereby allowing an assessment of the likelihood that life or habitable conditions exist there.

Types of Stars: On astrophysical grounds, Earth-like planets are likely to be found around stars that are roughly similar to the Sun (Turnbull 2004). Therefore, target stars will include main sequence F, G, and K stars. However, M stars may also harbor habitable planets, and the nearest of these could be investigated.

Terrestrial Planets: Considering the radii and albedos or effective temperatures of Solar System planets, the mission must be able to detect terrestrial planets, down to a minimum terrestrial planet defined as having 1/2 Earth surface area and Earth albedo. In the infrared, the minimum detectable planet would be one with an infrared emission corresponding to the surface area and optical albedo, positioned in the orbital phase space stipulated below and illustrated in Fig. 4-4.

Habitable Zone: A flagship mission should search the most likely range as well as the complete range of temperatures within which life may be possible on a terrestrial-type planet. In the Solar System, the most likely zone is near the present Earth, and the full zone is the range between Venus and Mars. The habitable zone (HZ) is here defined as the range of semi-major axes from 0.7 to 1.5 AU scaled by the square root of stellar luminosity (Kasting et al. 1993; Forget & Pierrehumbert 1997). The minimum terrestrial planet must be detectable at the outer edge of the HZ.

Orbital Phase Space: The distribution of orbital elements of terrestrial type planets is presently unknown, but observations suggest that giant-planet orbits are distributed roughly equally in semi-major axis, and in eccentricity up to those of the Solar System planets and larger. Therefore, a flagship mission must be designed to search for planets drawn from uniform probability distributions in semi-major axis over the range 0.7 to 1.5 AU and in eccentricity over the range 0 to 0.35, with the orbit pole uniformly distributed over the celestial sphere with random orbit phase.

Giant planets: The occurrence and properties of giant planets may determine the environments of terrestrial planets. The field of view and sensitivity must be sufficient to detect a giant planet with the radius and geometric albedo or effective temperature of Jupiter at 5 AU (scaled by the square root of stellar luminosity) around at least 50% of its target stars. A signal-to-noise ratio of at least 5 is required.

Exozodiacal dust: Emission from exozodiacal dust is both a source of noise and a legitimate target of scientific interest. A flagship mission must be able to detect planets in the presence of zodiacal clouds at levels up to a maximum of 10 times the brightness of the zodiacal cloud in the Solar System. Although the average amount of exo-zodiacal emission in the "habitable zone" is not yet known, we adopt an expected level of zodiacal emission around target stars of 3 times the level in our own Solar System with the same fractional clumpiness as our Solar System's cloud. From a science standpoint, determining and understanding the properties of the zodiacal cloud is essential to understanding the formation, evolution, and

habitability of planetary systems. Thus, the mission should be able to determine the spatial and spectral distribution of zodiacal clouds with at least 0.1 times the brightness of the Solar System's zodiacal cloud.

Spectral range: The required spectral range of the mission for characterization of exoplanets will emphasize the characterization of Earth-like planets and is therefore set to 6.5 to 18 μm in the infrared. The minimum range is 6.5 to 15 μm.

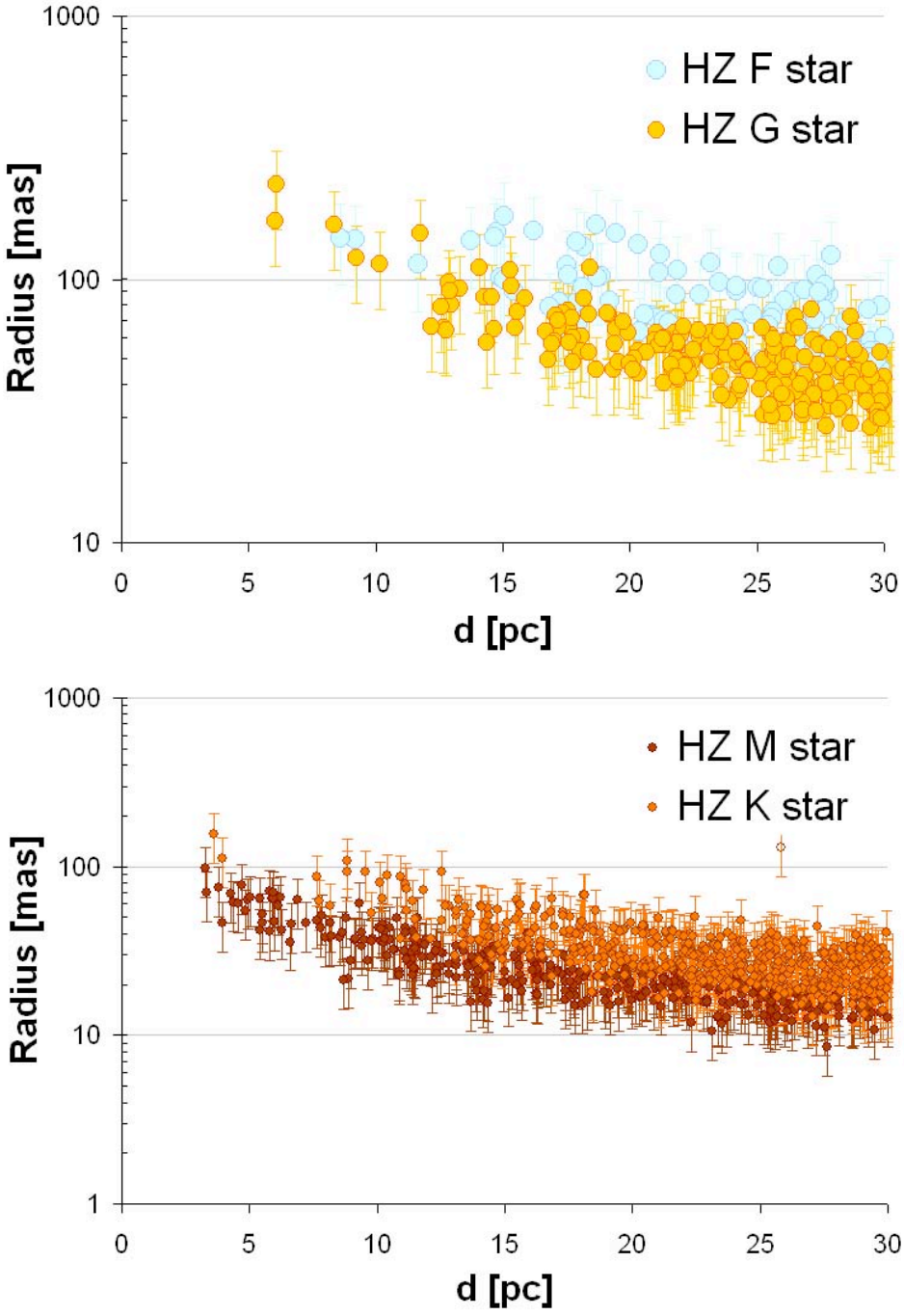

Figure 4-4. The extent of the Habitable Zone for the single main-sequence stars (F and G stars on upper panel, and M, K stars on lower panel) within 30pc from the Sun. (Kaltenegger et al. 2009)

Spectrum: The mission will use the spectrum of a planet to characterize its surface and atmosphere. The spectrum of the present Earth, scaled for semi-major axis and star luminosity, is used as a reference and suggests a minimum spectral resolution of 25 with a goal of 50. The mission must measure water (H_2O) and ozone (O_3) with 20% accuracy in the equivalent width of the spectral feature. Additionally it is highly desirable that the mission be able to measure carbon dioxide (CO_2) as well as methane (CH_4) (if the latter is present in high quantities predicted in some models of pre-biotic, or anoxic planets, e.g., Kasting & Catling 2003).

Table 4-1. Flagship Infrared Imaging Mission Requirement Summary

Parameter	Requirement
Star Types	F, G, K, selected, nearby M, and others
Habitable Zone	0.7–1.5 (1.8) AU scaled as $L^{1/2}$ *(Note *)*
Number of Stars to Search	> 150
Completeness for Each Core Star	90%
Minimum Number of Visits per Target	3
Minimum Planet Size	0.5–1.0 Earth Area
Geometric Albedo	Earth's
Spectral Range and Resolution	6.5–18 μm; R = 25 [50]
Characterization Completeness	Spectra of 50% of Detected or 10 Planets
Giant Planets	Jupiter Flux, 5 AU, 50% of Stars
Maximum Tolerable Exozodiacal Emission	10 times Solar System Zodiacal Cloud

*There are two definitions in the literature for the outer limit of the habitable zone. The first is 1.5 AU scaled to the luminosity to the ½ power based on Kasting et al. (1993). The second is 1.8 AU scaled in the same way from Forget & Pierrehumbert (1997).

Number of stars to be searched: To satisfy its scientific goals, the mission should detect and characterize a statistically significant sample of terrestrial planets orbiting F, G, and K stars. Although at this time, the fractional occurrence of terrestrial exoplanets in the Habitable Zone is not known, a sample of 150 stars within 30 pc (including a small number of nearby M stars) should suffice based on our present understanding.

Extended number of stars: It is desired to search as many stars as possible, beyond the required core sample. We anticipate that any mission capable of satisfying these objectives will also be capable of searching many more stars if the overall requirements on completeness are relaxed. It is desired that the mission be capable of searching an extended group of stars defined as those systems of any type in which all or part of the continuously habitable zone (see below) can be searched.

Search completeness: Search completeness is defined as that fraction of planets in the orbital phase space that could be found within instrumental and mission constraints. We require each of the 150 stars to be searched at the 90% completeness level. For other targets in addition to the 150 stars, the available habitable zone will be searched as to limits in planet's orbital characteristics.

Characterization completeness: While it will be difficult to obtain spectra of the fainter or less well positioned planets, we require that the mission be capable of measuring spectra of at least 10 (~50%) of the detected planets.

Visitations: Multiple visits per star will be required to achieve required completeness, to distinguish it from background objects, to determine its orbit, and to study a planet along its orbit. The mission must be capable of making at least three visits to each star to meet the completeness and other requirements.

Multiple Planets: After the completion of the required number of visitations defined above, the mission should be able to characterize a planetary system as complex as our own with three terrestrial-sized planets assuming each planet is individually bright enough to be detected.

Orbit Determination: After the completion of the required number of visitations defined above, the mission shall be able to localize the position of a planet orbiting in the habitable zone with an accuracy of 10% of the semi-major axis of the planet's orbit. This accuracy may degrade to 25% in the presence of multiple planets.

4.2 Observatory Concepts

An interferometer is a compelling choice for the overall design of a flagship mission. At mid-infrared wavelengths the angular resolution needed to resolve an Earth-Sun analog at a distance of 10 pc, would be ~50 mas, so that a conventional single-telescope design would need a primary mirror with a diameter larger than 40 m. By using separated apertures, baselines of hundreds of meters are possible. Nulling interferometry is then used to suppress the on-axis light from the parent star, whose photon noise would otherwise overwhelm the light from the planet (Bracewell 1978). Off-axis light is modulated by the spatial response of the interferometer: as the array is rotated, a planet produces a characteristic signal, which can be deconvolved from the resultant time series (Bracewell 1978; Léger et al. 1996; Angel & Woolf 1997). Images of the planetary system can be formed using an extension of techniques developed for radio interferometry (Lay 2005).

A probe-scale mission would have collecting apertures deployed on a single 'structurally-connected' spacecraft, and a flagship mission would have the very large formation-flying systems to achieve the strategic goals of life detection and planet imaging. We briefly describe concepts for both a small structurally connected interferometer and a larger formation-flying system.

4.2.1 Probe-Scale Mission Concept

Structurally-Connected Interferometer

An example of a small structurally-connected infrared interferometer concept is the Fourier-Kelvin Stellar Interferometer (FKSI), which is a two-telescope passively cooled nulling interferometer operating with observing wavelengths between 3 and 8 μm (see Danchi et al. 2003a,b), shown in Figure 4-5. The FKSI observatory will operate at the second Sun-Earth Lagrange point (L2) in a large amplitude Lissajious (or halo) orbit. The baseline design employs 0.5-m apertures. The telescopes employ two flat mirrors (siderostats) mounted 12.5 m apart on composite support booms, minimizing alignment requirements for the beams that enter the instrument package. The booms support sunshades that allow passive cooling of the structure to 60–65 K, reducing thermal noise in the telescope system

to a level that is negligible compared to that from the local zodiacal cloud (zodiacal background limited performance) over most of the instrument passband.

The mechanical design is appropriate for the smallest of the the Atlas V launch vehicles with a 4-m diameter fairing. The design minimizes the number of deployments. The deployments are listed as follows: (1) and (2) the two siderostats mounted on the ends of the booms, separated by 12.5 m, deployed using the well proven MILSTAR hinge technology. The booms are made from composite structures for an optimal strength-to-weight ratio, and the fixed sunshades are mounted to them; (3) a high-gain gimbaled S-band antenna for the data downlink; (4) a solar array for power; and (5) a radiator.

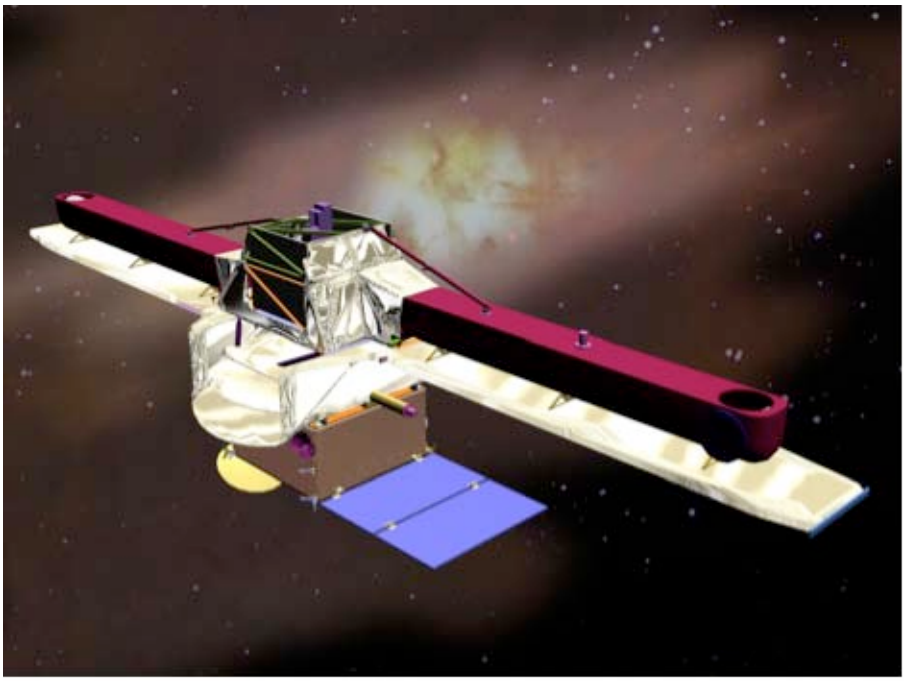

Figure 4-5. A small structually-connected interferometer mission concept. Two telescopes and passive cooling are used for observations in the 3–8 μm band. (W. C. Danchi, NASA GSFC)

A schematic diagram of the optical design is shown in Figure 4-6. There are five major subsystems in the instrument payload, which is mounted through a low-mechanical-frequency coupling and gamma-Al struts to the spacecraft bus. These include: (1) the boom-truss assembly that holds the siderostat mirrors and the non-deployed sunshields; (2) the main instrument module and optical bench assembly, which includes a pair of off-axis parabolic mirrors for afocal beam size reduction, and also a fast steering mirror assembly for the control of fine pointing, two optical delay lines (one to be used, the other is a spare), and two dichroic beam splitters, one for the angle tracker and fringe tracker assemblies (0.8–2.5 μm), the other for the science band of 3–8 μm; (3) the angle tracker assembly for fine pointing; (4) the fringe tracker assembly for stabilizing the fringes for the nulling instrument assembly; and (5) the nulling instrument assembly itself.

The nulling instrument is based on a modified Mach-Zehnder beamsplitter design that maximizes the symmetry of the two beams, helping to ensure a deep null. Other elements in the system include shutters for alignment and calibration purposes, an assembly for amplitude control of the fringe null, and optical fibers for wavefront cleanup. The fibers help achieve the desired null depth with reduced tolerances on the preceding optical

components (in order to reduce manufacturing costs). The dark and bright outputs are sent to their respective Focal Plane Arrays (FPAs), which could be long wavelength HgCdTe arrays from Teledyne (previously Rockwell) operating at 35 K, or Si:As arrays operating at 8 K, based on those for the MIRI instrument on *JWST*. The FPAs for the fringe and angle trackers are operated at 77 K and are based on the HgCdTe arrays used on the NICMOS instrument on *HST*. Cryogenic delay lines are used to equalize the pathlengths between the two sides of the interferometer.

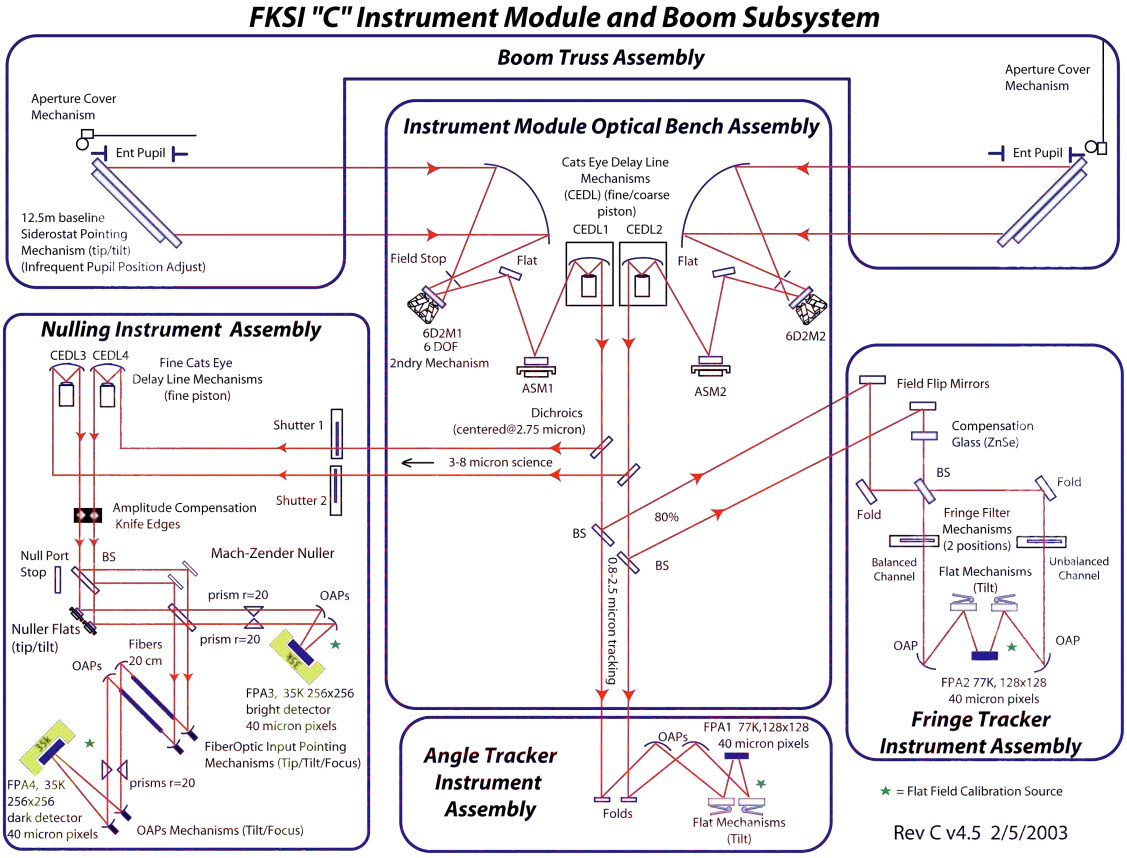

Figure 4-6. Schematic design of the boom and instrument module subsystem for FKSI. The various subassemblies are as noted in the figure. (W. C. Danchi, NASA GSFC)

When the instrument is in operation, it rotates slowly around the line of sight to the object. In so doing, a periodic signal is generated at the output of the nuller instrument, which is non-zero if there is a planet or spatially resolved source within the transmission pattern of the nuller. Data from the bright port is also taken providing measurements of the visibility of the object. Simulations have been performed, both for nulling operation as well as imaging (Danchi et al. 2003a; Barry et al. 2005, 2006). Table 4-2 lists the types of measurements that can be made with such as system; the companion figure, Figure 4-2, shows that a small interferometer is capable of measuring the emission spectra of known exoplanets with a large range of semi-major axes.

The concept discussed above has undergone a thorough integrated analysis and modeling study of the structure and optics to validate the design and ensure it meets requirements (Hyde et al. 2004). A major concern was the propagation of reaction-wheel disturbances from the spacecraft bus through the bus-instrument package coupling up to the boom system. Contributions to the performance error budget for the required 10^{-4} null are well

understood and have been reported in Hyde et al. (2004). The null depth requirement drives the instrument performance. Other sources of noise include the Fringe Tracker (FT), the Optical Delay Line (ODL), the Attitude Control System (ACS), and the booms themselves. The boom system had the lowest order modes at 5.6 and 7.3 Hz. This modeling verified that the closed-loop performance requirement could be met or exceeded at all wheel speeds from 0.1 to 100 Hz (Hyde et al. 2004).

Performance

Table 4-2 lists the planetary characteristics and what can be determined using a modest nulling interferometer. This list includes planetary temperature, radius, mass density, albedo, surface gravity, and atmospheric composition, as well as the presence of water. To date, progress has been made on the physical characteristics of planets largely through transiting systems, but a small planet-finding interferometer can measure the emission spectra of a large number of the non-transiting ones, as well as more precise spectra of the transiting ones.

Table 4-2. Characteristics of exoplanets that can be measured using FKSI

Parameters	What FKSI Does
Removes sin(i) ambiguity	Measure
Planet Characteristics	
Temperature	Measure
Temperature variability due to distance changes	Measure
Planet radius	Measure
Planet mass	Estimate
Planet albedo	Cooperative
Surface gravity	Cooperative
Atmospheric and surface composition	Measure
Time variability of composition	Measure
Presence of water	Measure
Planetary System Characteristics	
Influence of other planets, orbit co-planarity	Estimate
Comets, asteroids, zodiacal dust	Measure

Many molecular species (such as carbon monoxide, methane, and water vapor) have strong spectral features in the 3–8 μm region, as can be seen in Figure 4-2, which displays model atmospheres for exoplanets calculated by Seager (2005), for planets at various distances from the host star. The red curve shows the theoretical spectrum of a very hot, close-in planet at 0.05 AU, while the blue curve displays spectrum for a much cooler planet ten times further out, at 0.5 AU. Also displayed are sensitivity curves for the IRAC instrument on *Spitzer* (light blue) and FKSI (purple). Clearly such a mission concept has sufficient sensitivity to detect and characterize a broad range of exoplanets.

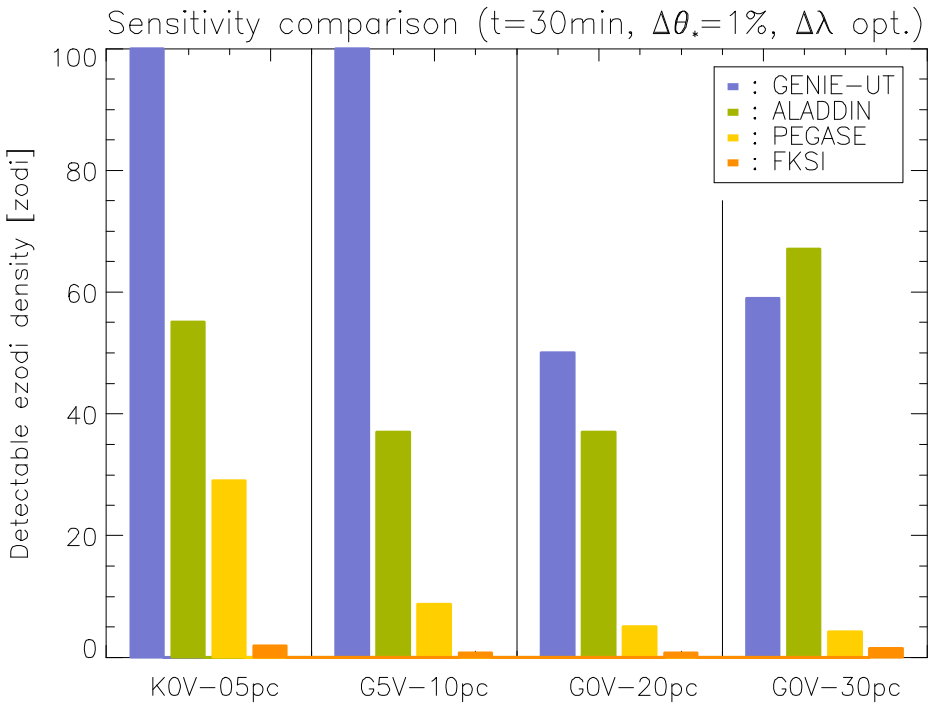

Figure 4-7. Expected performance for Pegase and FKSI compared to the ground-based instruments, for 30 min integration time and 1% uncertainty on the stellar angular diameters. (Defrère et al. 2008)

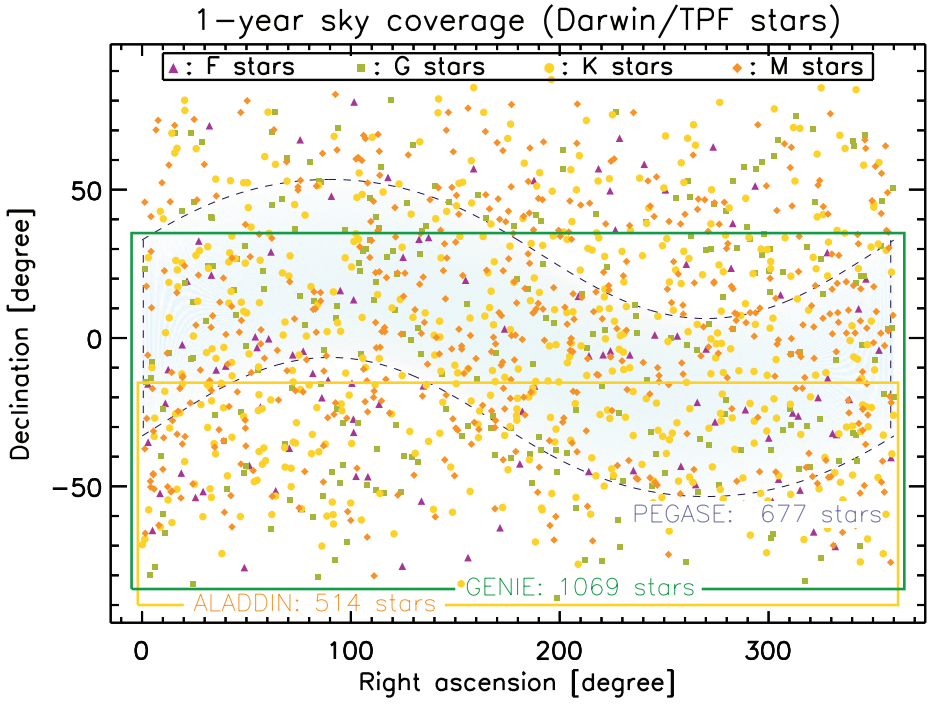

Figure 4-8. Sky coverage after 1 year of observation of GENIE (dark frame), ALADDIN (light frame) and Pegase (shaded area) shown with the Darwin/TPF all sky target catalogue. The blue-shaded area shows the sky coverage of a space-based instrument with an ecliptic latitude in the [−30°,30°] range (such as Pegase). The sky coverage of FKSI is similar to that of Pegase with an extension of 40° instead of 60°. (Defrère et al. 2008)

Initial studies with very conservative assumptions of an 8-m boom length, 140 exoplanets (known at that time), 120-s on-source integration time, 15-nm RMS path length error, telescope temperature of 65 K, and a small sunshield with a ±20 degree field of regard; gave ~25 detections. Currrently, there are about 250 known planets, so with those assumptions and the same detection ratio of about 18%, it should be possible to detect and characterize about 45 exoplanets, and a larger sunshade with a field of regard of ± 45 degrees would approximately double this number to ~90 planets.

Recent studies of the detectability of debris disks (Defrère et al. 2008) demonstrated that the residual pathlength error for a small system like FKSI should be of the order of 2 nm RMS, which would significantly increase the number of exoplanets. As a conservative estimate, we expect that a small system could detect (e.g., remove the sin(*i*) ambiguity) and characterize about 75–100 known exoplanets.

These recent studies also have shown that a small mission is ideal for the detection and characterization of exozodial and debris disks around *all* candidate target stars in the Solar neighborhood as seen in Figures 4-7 and 4-8. (Defrère et al. 2008). Indeed, the performance level of the FKSI system is of the order of 1 Solar System Zodi in 30 minutes of integration for a G0 star at 30 pc. With a small sunshade, this system could observe of the order of 450 stars in the Solar neighborhood, and with a larger field-of-regard, such as ± 45 degrees, the exozodis and debris disks of about 1000 stars could be studied.

Although the telescopes are somewhat larger than has been discussed in some of the existing mission concepts (e.g., 1–2 m) and are somewhat cooler (e.g., < 60 K) so that the system can operate at longer wavelengths, it is possible for a small infrared structurally connected interferometer to detect and characterize Super Earths and even ~50–75 Earth-sized planets around the nearest stars. This is especially important now that there is evidence that lower mass planets may be very common, based on the detection of the 5.5-Earth-mass planet using the microlensing approach (e.g., Beaulieu et al. 2006; Gould et al. 2006).

Further studies of the capabilities of a small infrared structurally-connected interferometer are necessary to improve upon our estimates of system performance.

4.2.2 Flagship Mission Concept

Formation Flying Interferometer

Figure 4-9 depicts a mission concept capable of detecting a large number of Earth-sized planets. This Emma X-Array formation-flying design is the culmination of more than a decade of study by NASA and ESA. Light from the target star is reflected from the four collector mirrors (~2 m diameter) and focused onto the input apertures of the combiner spacecraft approximately 1 km away. To observe a target system, the collector array is rotated slowly about the line-of-sight, using a combination of centimeter-precision formation flying and careful attitude control to maintain the pointing of the beams. The light entering the combiner passes through a series of optics (Figure 4-10) that performs beam steering and compression, delay compensation, intensity and dispersion correction (see "the Adaptive Nuller" below), pairwise beam combination with π phase shift (the nullers), cross-combination of the nulled beams, single-mode spatial filtering, and, finally, dispersion and detection of the nulled light on the science camera. The time series of output data is synthesized into an image. A key advantage of the X-Array configuration is its very high angular resolution, as illustrated by the simulated image shown in Figure 4-11.

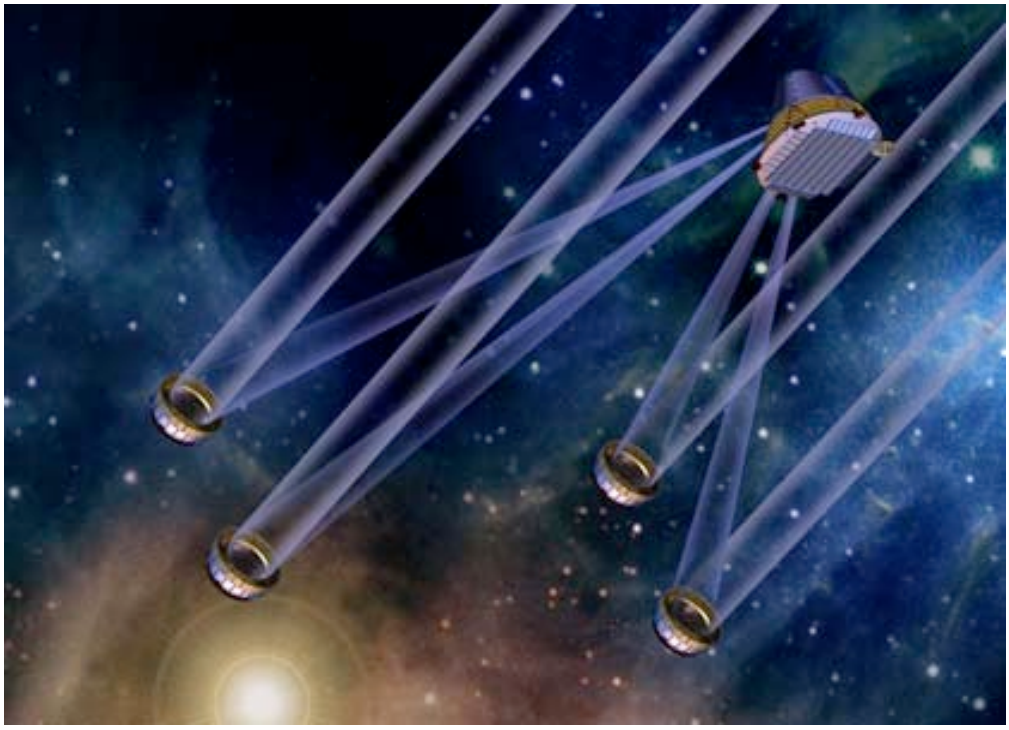

Figure 4-9. 'Emma X-Array' formation flying concept.

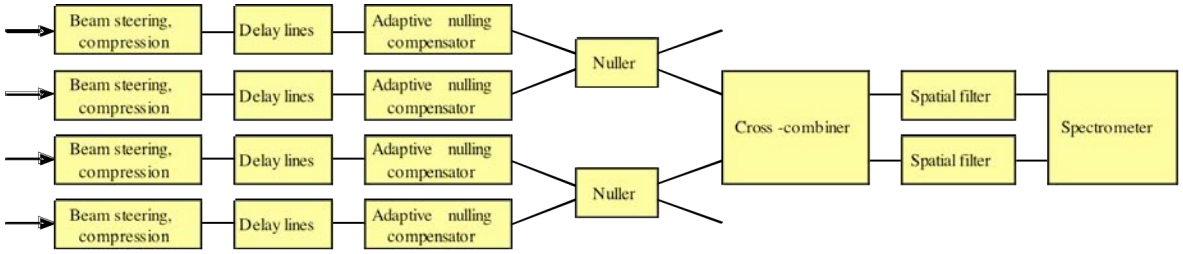

Figure 4-10: Schematic of beam combiner optics.

Performance

The planet-finding capability for a formation-flying Emma X-Array design is shown in Figure 4-12. A mission with 2-m diameter collectors would be capable of detecting more than 100 Earth-sized planets around nearby stars, primarily F, G, and K spectral type, over a period of 2 years, assuming $\eta_{\oplus} = 1$. The performance model is described in Lay et al. (2007) and includes the dominant sources of noise: photon noise from local zodi, exo-zodi and stellar leakage, and instability noise (Lay 2004) from fluctuations in the phasing and intensity balance within the instrument optics. Following a candidate planet detection and follow-up confirmation, a longer period of observing time is dedicated to spectroscopic characterization, using the same observing procedure as for the initial detection. Details of a design study for the array are given by Martin et al. (2008a).

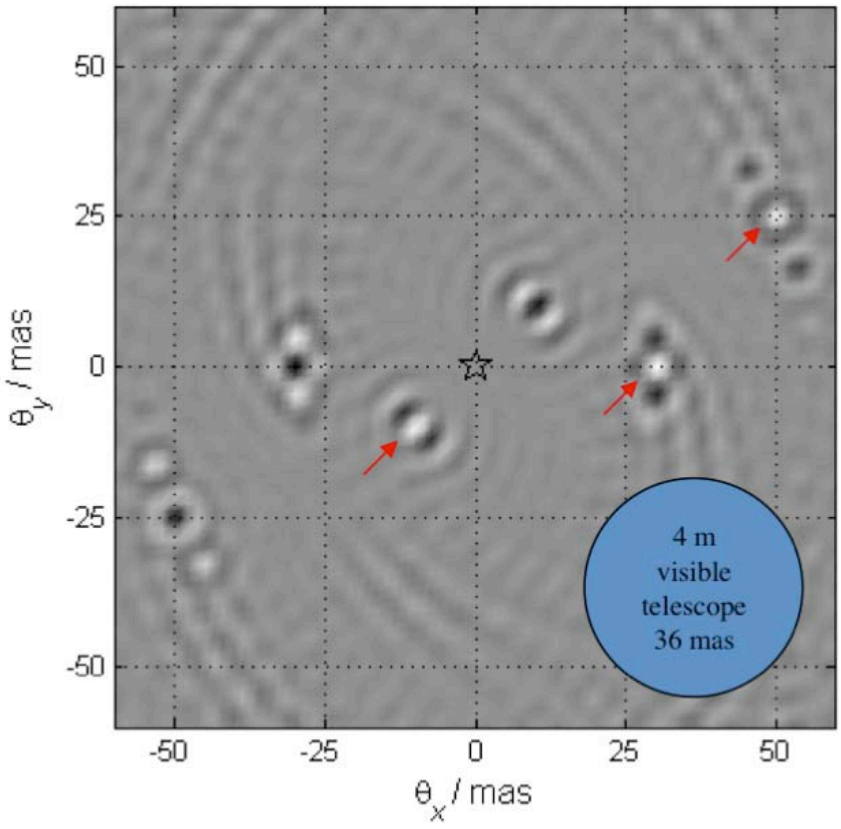

Figure 4-11: Simulated 'dirty' image from a 400 × 67-m Emma X-Array, prior to deconvolution. Angular resolution is 2.5 mas. Planet locations are indicated by red arrows. Simultaneous full resolution (R ~ 100) spectroscopy for all objects within the field of view is a natural by-product of interferometric observing. While data from the detection and orbit-determination phases should be sufficient for a coarse spectrum, a deep characterization will require significant integration time. Detection of CO_2 for an Earth at 5 pc using 2-m collectors will require ~24 hours of integration (SNR of 10 relative to the continuum). The narrower ozone absorption line requires 16 days at 5 pc. For ozone at 10 pc, integration times as long as 40 days could be needed, falling to ~6 days with 4-m diameter collectors. (O. P. Lay, JPL)

4.3 Technology

4.3.1 Experiments in Nulling Interferometry, 1999–2009

Results obtained in the lab have met the requirements for infrared nulling needed for a probe-scale mission and are close to meeting those of a flagship mission. Laboratory work with the Adaptive Nuller has indicated that mid-infrared nulls of 1.0×10^{-5} are now achievable with a bandwidth of 34% and a mean wavelength of 10 μm; this suggests that at the subsystem-level the nulling performance for a flagship mission is near TRL 4 (cryogenic testing would be needed for TRL 5). These results also show that the achromatic phase shifters, the Adaptive Nuller, and the mid-infrared single-mode fibers that are contributing to these results are now mature technology. A summary of the past decade's research in nulling interferometry is given in the paragraphs that follow.

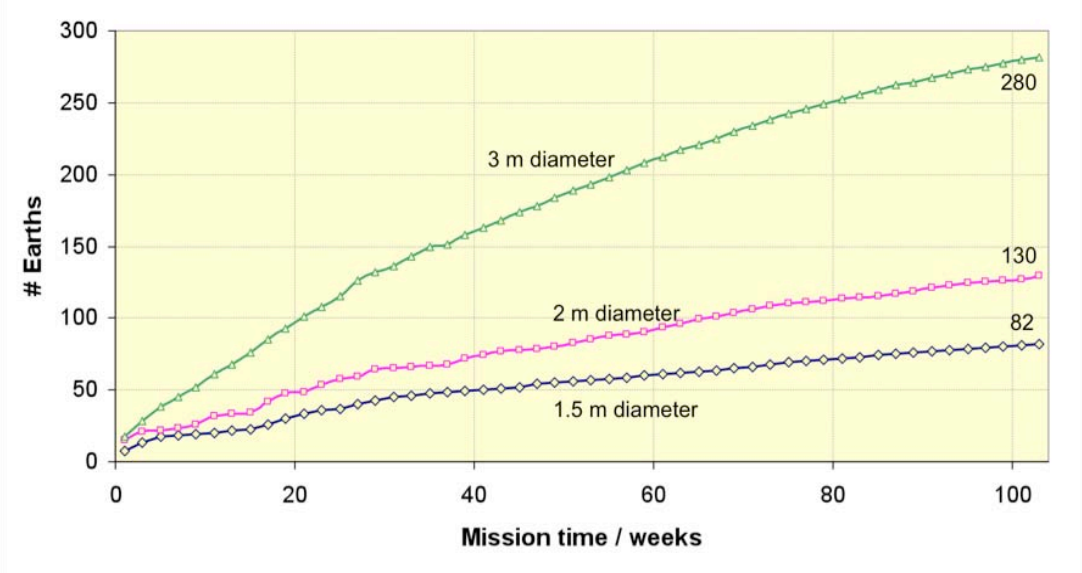

Figure 4-12: Predicted number of Earths detectable by Emma X-Array architecture as a function of elapsed mission time and collector diameter. (O. P. Lay & S. Hunyadi, JPL)

Deep nulls of narrowband light have been achieved using both pupil-plane and focal plane nulling techniques, and the extension of these results to broadband and randomly polarized sources is now the remaining challenge. To achieve deep nulls in an interferometer, the optical properties of the combined beams must be quite similar. The properties include intensity balance, polarization angle, polarization dispersion, and wavefront differences. Some of the requirements for the balance in these properties can be mitigated by the use of single-mode spatial filtering at the detector, for example by using a single-mode fiber to receive the light. The components of the optical system will introduce defects into the pristine wavefront received from the stellar source, adding wavefront deformations and polarization changes. If these defects are more or less the same in each input beam of the interferometer, the system will still be capable of nulling. For a broadband source, the effects of the defects need to be controlled across the entire nulling waveband, and this requirement has been addressed with the development of the Adaptive Nuller (Peters et al. 2008), which is a system designed to correct intensity and phase differences across the band for both polarizations.

Since 1999 when Ollivier (1999) reported laser nulls of ~1.7×10^{-4} and Serabyn (1999) reported 5.0×10^{-5}, progress has been made in both null depth and bandwidth. Deep, single-polarization laser nulls in the mid-infrared waveband of order 3.0×10^{-6} were reported by Martin et al. (2003), and Samuele et al. (2007) reported nulls of order 1.1×10^{-7} at visible wavelengths. Similarly, since Wallace et al. (2000) reported broadband nulls of 7.4×10^{-5} at 18% bandwidth, Samuele et al. (2007) achieved 1.0×10^{-6} at 15% bandwidth in the visible and Peters et al. (2008) have shown through narrowband measurements that 1.0×10^{-5} nulls at 34% bandwidth in the mid-infrared are attainable. These results and others of note are included in Figure 4-13, which illustrates the experiments undertaken since 1999.

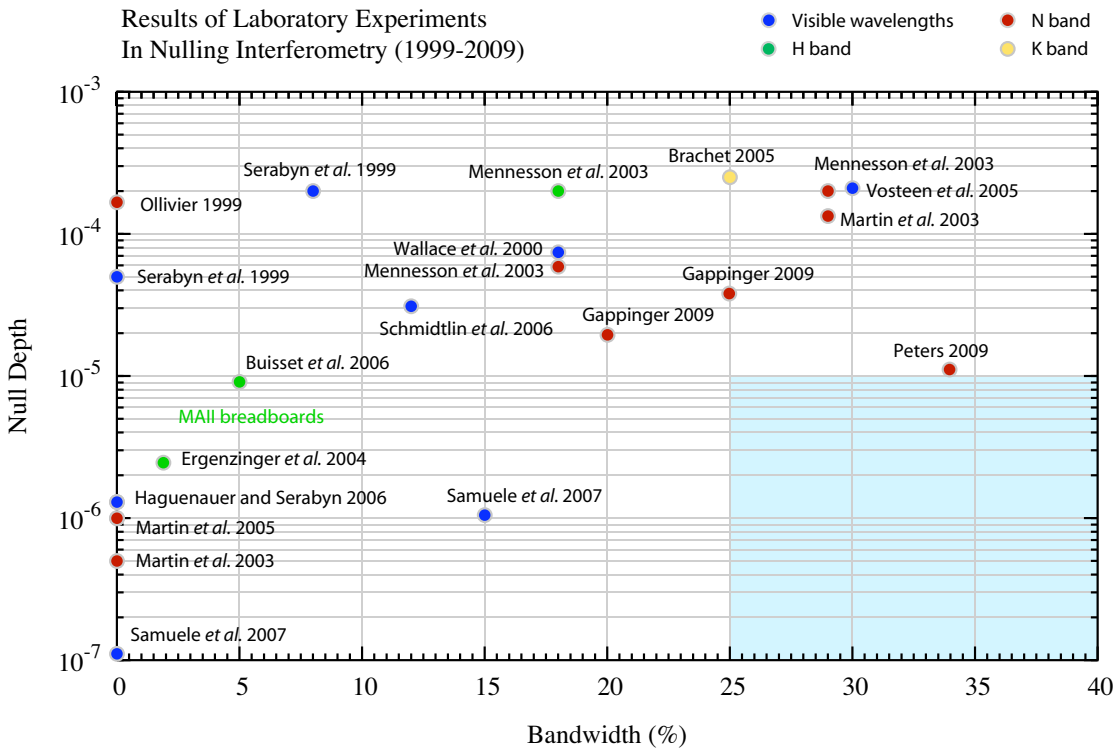

Figure 4-13. Chart of null depths achieved since 1999. The blue shaded area highlights the nulling performance needed to be demonstrated in the lab in preparation for a flagship mission. (P. R. Lawson, JPL)

Serabyn's early nuller, known as the SIM roof-top nuller, was used for both laser and broadband nulling tests near the visible waveband. It used a geometric field inversion technique but was asymmetric in that a beamsplitter-compensator plate arrangement was used. A more symmetrical nuller was then built for the Keck telescopes, the modified Mach-Zehnder (MMZ) nuller (Crawford et al. 2005) in which field inversion was performed outside the nuller and the beams traversed two beam splitters each, allowing symmetrical treatment (Figure 4-14).

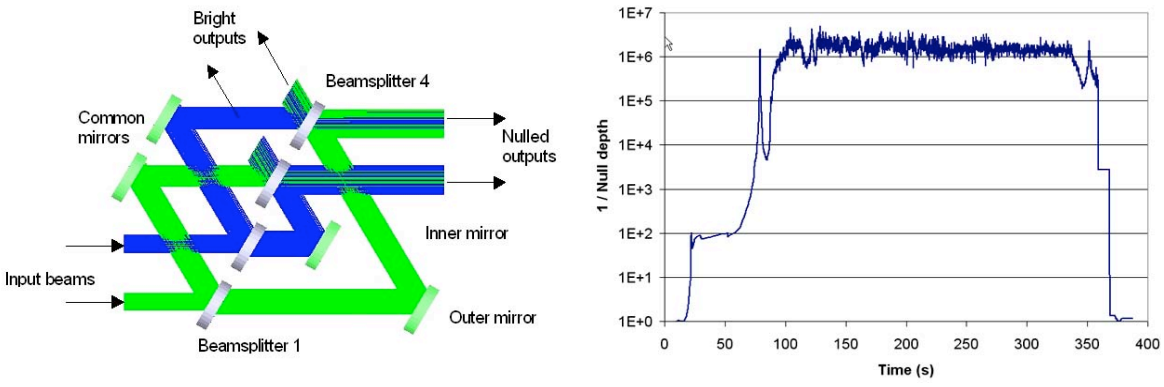

Figure 4-14. (left) MMZ nuller built for Keck telescopes, (right) single-polarization laser null at 10.6 μm showing null depth of 5×10^{-7}.

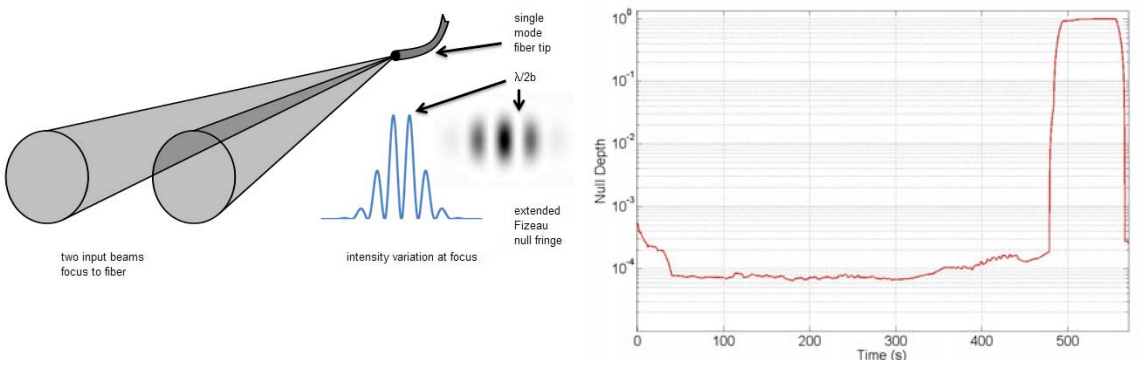

Figure 4-15. (left) concept for a nuller using a fiber beam combiner, (right) unpolarized broadband null of 18% bandwidth at 1.65 mm showing null depth better than 1 × 10–4.

The Keck nuller (Serabyn et al. 2004) employs two MMZ nullers to null four input beams and operates in the mid-infrared. More recently, laboratory work has used Mach-Zehnder schemes to produce symmetrical nulling systems for the Planet Detection Testbed (PDT) (Martin et al. 2006) and the Achromatic Nulling Testbed (ANT) (Gappinger et al. 2009), for example. The PDT has nulled four laser beams at 10.6 μm wavelength at the 2.5×10^{-5} level.

A somewhat different interferometric beam-combination scheme has also been proposed in Europe (Wallner et al. 2004; Karlson et al. 2004). By combining beams directly on a single-mode fiber, the complex interaction of the light with beamsplitter and antireflection coatings can be eliminated. Conceptually, such a beamcombiner can be both achromatic and polarization insensitive, at the cost of some optical throughput efficiency. Small-scale testbeds for this type of beamcombiner are being developed and have achieved deep laser nulls of 2.0×10^{-4} (Mennesson et al. 2006) in the visible and broadband nulls of order 1.0×10^{-4} at 18% bandwidth at J-band (Martin et al. 2008b) (Figure 4-15).

4.3.2 Technology for Probe and Flagship Missions

Mid-IR Spatial Filters

Spatial filters are an essential technology for nulling interferometry. They can be used to reduce complex optical aberrations in the incoming wavefronts to simple intensity and phase differences (which are more readily corrected), thus making extremely deep nulls possible. Spatial filters may be implemented in a variety of ways, including single-mode fiber-optics made from chalcogenide glasses, metallized waveguide structures micro-machined in silicon, or through the use of photonic crystal fibers. Two types of fiber spatial filters have been successfully developed: polycrystaline silver halide fibers have been developed by Prof. Abraham Katzir at Tel Aviv University (TAU) in Israel; and chalcogenide fibers have been developed by Dr. Jas Sanghera at the Naval Research Laboratory (NRL).

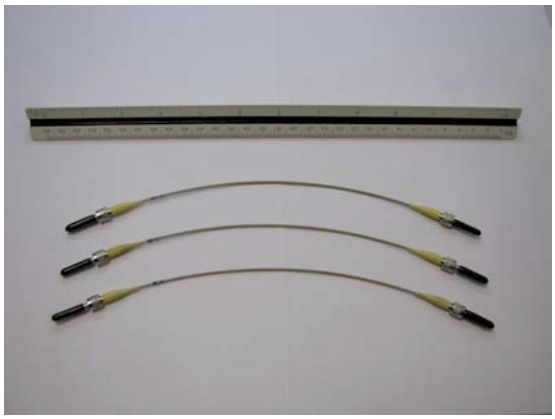

Figure 4-16. Single-mode Chalcogenide fibers developed by the Naval Research Laboratory

The 20-cm long chalcogenide fibers developed by the Naval Research Laboratory (shown in Figure 4-16) were shown to demonstrate 30-dB rejection (a factor of 1000) of higher order modes and have an efficiency of 40%, accounting for both throughput and Fresnel losses (Ksendzov et al. 2007). The transmission losses were measured to be 8 $dB \cdot m^{-1}$, and the fibers are usable up to a wavelength of about 11 μm. The chalcogenide fibers developed at the Naval Research Laboratory were used successfully in the Achromatic Nulling Testbed and are currently in use in the Adaptive Nuller testbed.

The 10–20 cm long silver halide fibers that were developed by Tel Aviv University were shown to demonstrate 42-dB rejection (a factor of 16,000) of higher order modes with transmission losses of 12 dB m^{-1} (Ksendzov et al. 2008). This high rejection of higher-order modes was accomplished with the addition of aperturing of the output of the fibers, made possible by the physically large diameter of the fibers. Silver halide fibers should in principle be usable up to a wavelength of about 18 μm, although the lab tests at JPL were conducted only at 10 μm. This is the first time silver halide fibers were demonstrated to have single-mode behavior.

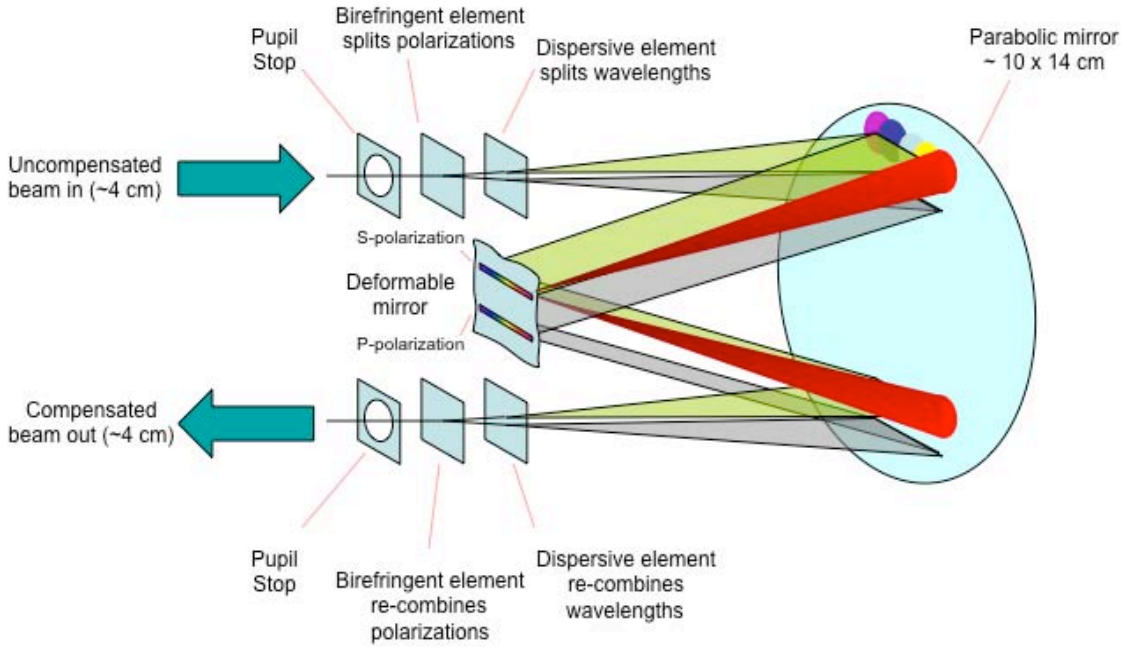

Figure 4-17. Schematic of the Adaptive Nuller. Uncompensated light that enters the device is split into two linear polarizations, and each polarizaion is treated separately then recombined. Light is dispersed and imaged onto a deformable mirror (DM). Piston of elements in the DM adjusts phase at a particular wavelength, and tilt of the same pixel adjusts relative intensity by shearing the output pupil at that wavelength.

Adaptive Nulling and Achromatic Phase Shifters

The variations in amplitude and phase that may be present in the incoming wavefront must be corrected in order to achieve deep nulls at every wavelength. The Adaptive Nuller was designed to correct phase and intensity variations as a function of wavelength, in each of two linear polarizations. In principle this should allow high-performance nulling interferometry, while at the same time substantially relaxing the requirements on the nulling interferometer's optical components. The goal of the testbed was to demonstrate, in a 3-μm band centered at a wavelength of 10 μm, the correction of the intensity difference to less than 0.2% RMS (1 σ) between the interferometer's arms, and at the same time correct

the phase difference across the band to < 5 nm RMS (1 σ). This overall correction is consistent with a null depth of 1×10^{-5} (1 part in 100,000) if all other sources of null degradation can be neglected.

The Adaptive Nuller was designed to correct these variations, matching the intensity and phase between the two arms of the interferometer, as a function of wavelength, for both linear polarizations. A deformable mirror is used to adjust amplitude and phase independently in each of about 12 spectral channels. A schematic of the adaptive nuller is shown in Figure 4-17. Two prisms split the incoming light into its two linear polarization components and divide it into roughly a dozen spectral channels. The light is then focused onto a deformable mirror where the piston of each pixel independently adjusts the phase of each channel. By adjusting the angle of the reflected beam so that the beam is slightly vignetted at an exit aperture, the intensity is also controlled. The adaptive nuller uses a broadband thermal source to generate light in the 8–12 μm wavelength band. A photograph of the testbed is shown in Figure 4-18.

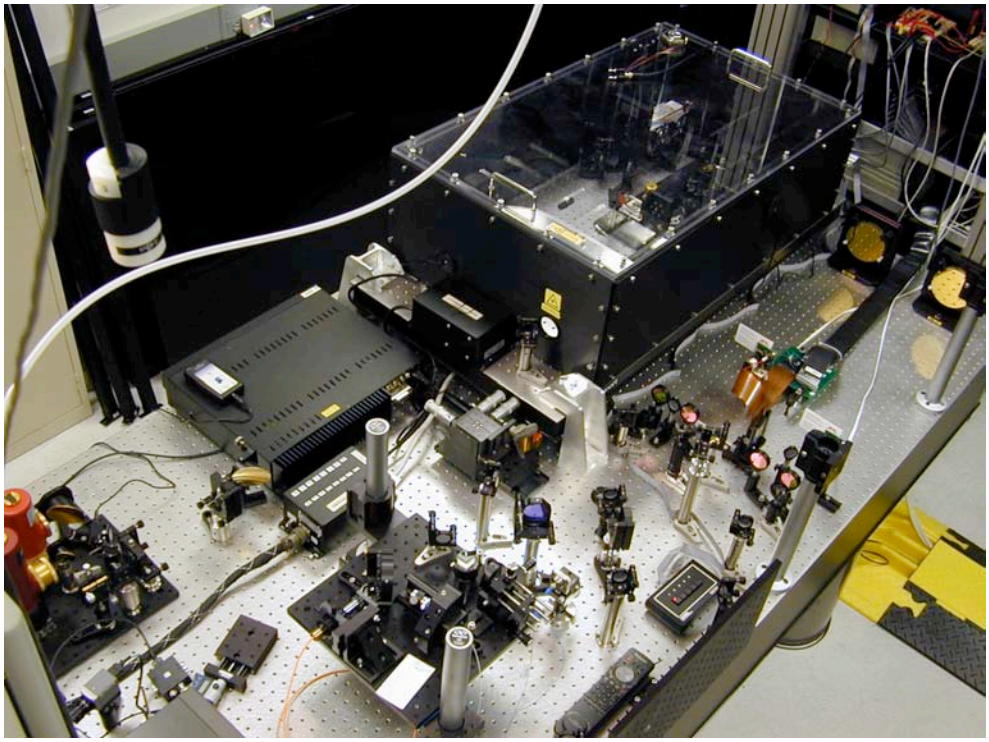

Figure 4-18. The Adaptive Nuller Testbed (AdN). The Adaptive Nuller demonstrated phase and intensity compensation of beams within a nulling interferometer to a level of 0.12% RMS in intensity and less than 5 nm RMS in phase. This version of the AdN operates over a wavelength range of 8–12 μm. The long-focus parabolas, used in AdN are seen on the upper right.

The initial results of this research have been published by Peters et al. (2008). In March/April 2007, the testbed achieved its primary goal of demonstrating phase compensation to better than 5 nm RMS across the 8–12 μm band and intensity compensation to better than 0.2% RMS. Narrow-band measurements of null depth in the channels across the passband indicated a null depth of 1.0×10^{-5}, would be attainable. When demonstrated using the full bandwidth of the Adaptive Nuller, it would be the deepest broadband null ever achieved by a mid-infrared nulling interferometer and would demonstrate the flight requirement for a flagship mission.

Cryocoolers

With the Advanced Cryocooler Technology Development Program (ACTDP), the Terrestrial Planet Finder (TPF) and *JWST* projects have produced development model coolers that have met or exceeded their performance requirements, which are to provide ~30 mW of cooling at 6 K and ~150 mW at 18 K. This demonstrates the approach to cooling the science detector to a temperature low enough to reveal the weak planet signals. This activity is at TRL 6.

Cryogenic delay lines

The Dutch company TNO Science and Industry led a consortium that developed a compact cryogenic Optical Delay Line (ODL) for use in future space interferometry missions such as ESA's Darwin and NASA's TPF-I (Figure 4-19). The prototype delay line is representative of a flight mechanism. The ODL consists of a two-mirror cat's eye with a magnetic bearing linear guiding system. TNO and its partners have demonstrated that accurate optical path-length control is possible with the use of magnetic bearings and a single-stage actuation concept. Active magnetic bearings are contactless, have no friction or hysteresis, are wear free, and have low power dissipation. The design of the Darwin broadband ODL meets the ESA requirements, which are an OPD stroke of 20 mm, stability of 0.9 nm RMS (with a disturbance spectrum of 3000 nm RMS, < 20 mW power dissipation (2 mW with flight cabling), output beam tilt < 0.24 microradians, output lateral shift < 10-μm peak-to-peak, wavefront distortion < 63 nm RMS at 40 K, and wavelength range (0.45–20 μm). The Darwin ODL is representative of a future flight mechanism, with all materials and processes used being suitable for flight qualification. Positioning is done with a voice coil down to subnanometer precision. The verification program, including functional testing at 40 K, has been completed succesfully. This technology is at TRL 6 (see Fridlund et al. 2008).

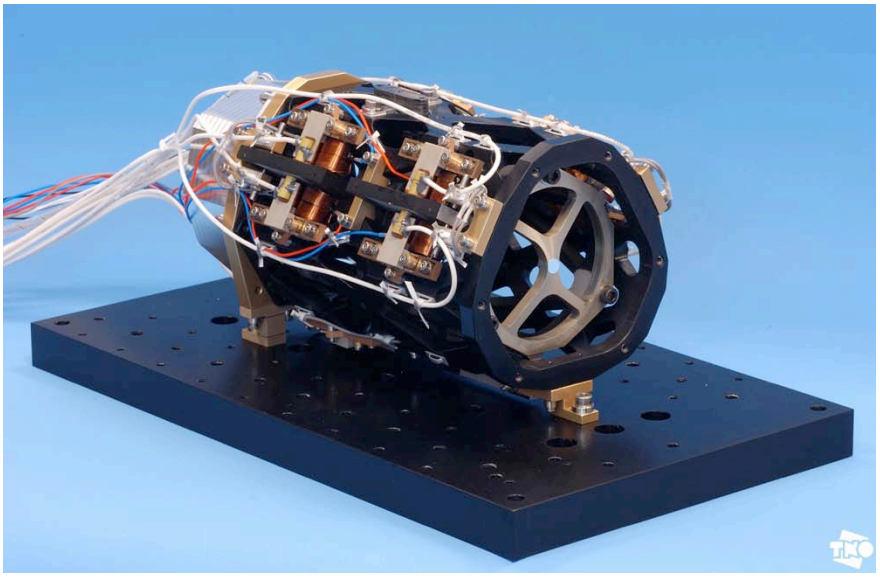

Figure 4-19. Overview of the Optical Delay Line with the outer fixed structure holding the active parts for magnetic levitation and axial motion, and the inner moving structure that includes the optical components. (Courtesy of ESA and TNO)

Thermal shields

Science requirements for *JWST* have driven the need for a deployable, low areal-density, high thermal-performance efficiency (effective emittance, e* of 10^{-4} to 10^{-5}) sunshield to passively cool the Observatory Telescope Elements and Integrated Science Instruments Module (OTE/ISIM). The thermal performance dictated the need for a sunshield consisting of multiple, space-membrane layers such that the ~200 kW of the Sun's energy impinging on the Sun-facing layer would be attenuated such that the heat emitted from the rear or OTE-facing membrane would be < 1 W. This would enable the OTE/ISIM to operate at cryogenic temperature levels (< 50 K) and have a temperature stability of 0.1 to 0.2 K over the field-of-regard pointing re-alignments.

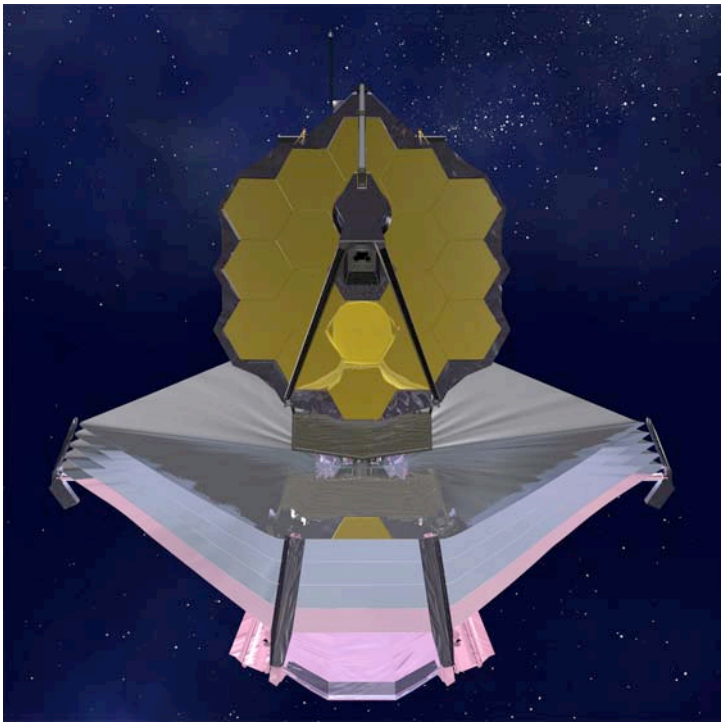

Figure 4-20. The James Webb Space Telescope. (Courtesy NASA/JWST)

Based on these top-level mission requirements a sunshield was developed employing five membrane layers with pitch and dihedral separation angles of 1.6 and 2 degrees, respectively. Through the use of a low solar absorptance-to-emittance ratio (α_S / ε_H) coating on the Sun-facing surface (layer 1) and an infrared highly reflective coating on the majority of the other membranes' surfaces, the Sun's heatload absorbed by the Sun-facing membrane is reduced and the resulting infrared energy re-emitted to the other layers would be reflected laterally out the open sides of the sunshield, thus greatly attenuating the residual infrared energy emitted by the OTE/SIM-facing membrane surface (layer 5). From a variety of trade studies the Sunshield evolved into a five-membrane system as shown in Figure 4-20 with membranes 140 to 150 m^2 in size that are supported by six spreader bar/boom assemblies and are lightly tensioned in a deployed configuration by constant-force spring-loaded catenary cable assemblies attached to the periphery of each membrane. The present sunshade design for *JWST* is at TRL 6 and meets the similar requirements for the flagship mission and is more than adequate for a small mission (Kurland 2007).

Detector Technology

Detectors or Sensor Chip Assemblies (SCAs) from the *JWST* Mid-Infrared Instrument (MIRI) have been developed by Raytheon Vision Systems (RVS) having 1024 × 1024 pixels fabricated from arsenic-doped silicon (Si:As) and which consist of a detector layer and a readout multiplexer. The detector structure is a backside-illuminated silicon substrate with an active-detector layer grown on top of that, followed by a blocking layer (to minimize the dark current), and then indium bumps. The readout multiplexer is a cryogenically optimized electronic circuit chip having a source follower (transistor) for each detector pixel, which then multiplexes those pixels down to four video outputs that are read by the remaining instrument electronics. The two components of the SCAs are mated together through matching indium bumps. The required performance levels are dark current less than 0.03 electrons per second, readout noise less than 19 electrons, and quantum efficiency > 50%. These detectors have been rigorously tested and have met or exceeded these requirements for *JWST*, giving a TRL of 6 (Ressler 2007). These detectors meet or exceed the requirements for both a small structurally connected interferometer mission and the flagship mission. See Figure 4-21 for an example of a complete focal plane module for the MIRI instrument on *JWST*.

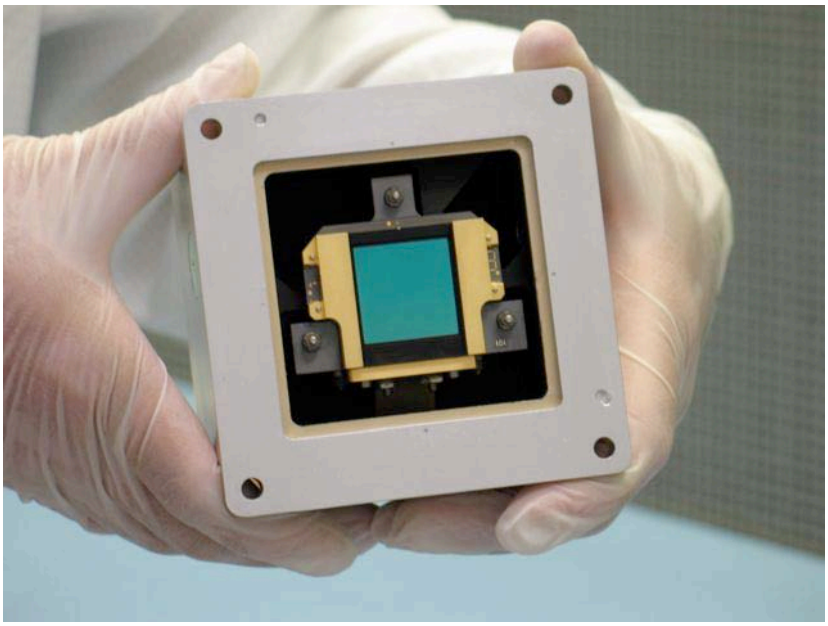

Figure 4-21. The MIRI Focal Plane Module contains the SCA, a fanout board, and the mounting structure needed to position and isolate the sensor. (Courtesy NASA/JWST)

Integrated Modeling

Observatory Simulation: Demonstrate a simulation of the flight observatory concept that models the observatory subjected to dynamic disturbances (e.g., from reaction wheels). Validate this model with experimental results from at least the Planet Detection Testbed at discrete wavelengths. Use this simulation to show that the depth and stability of the starlight null can be controlled over the entire waveband to within an order of magnitude of the limits required in flight to detect Earth-like planets, characterize their properties, and assess their habitability. This activity is at TRL 5 (Lawson et al. 2007).

4.3.3 Additional Technology for a Flagship Mission

Four-beam nulling: Dual-beam chopping and spectral filtering

The Planet Detection Testbed (PDT) is a breadboard system intended to demonstrate techniques that will be required for detection of exoplanets using a mid-infrared telescope array. As a breadboard system operating in a normal room environment, it differs from a flight-demonstration system in both its layout and in the flux levels that it uses, which are much higher than would be encountered in space. It does, however, embody the controls and sensors necessary for operation in space. Furthermore, the differences do not affect the key goal of the testbed, which is to demonstrate faint planet detection using nulling interferometry, phase chopping and averaging.

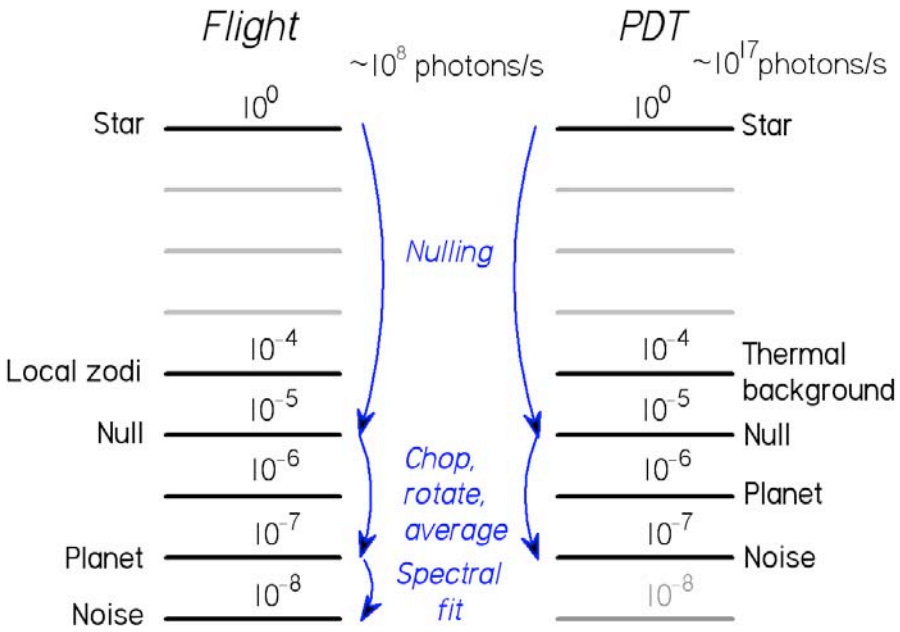

Figure 4-22. Photon rates for the planet detection process for flight and PDT.

Key exoplanet-detection techniques are being tested and demonstrated in the PDT. To reach the flight goal of detection of a planet 10^7 times fainter than the parent star, a series of steps (illustrated in Figure 4-22) must be taken:

- The star's apparent intensity is reduced relative to the planet by a factor of 100,000. This is done by interferometric nulling.
- The interferometer array is rotated around the line of sight to the star to search the whole region around the star for a characteristic planet signature. In the PDT this is done by controlling the optical path relationships between the planet source beams, simulating the phase changes caused by rotation of the telescope array around the line of sight to the star. During this rotation, stable nulls need to be maintained; the PDT has systems and control loops analogous to those needed for flight in order to control the instability noise and maintain deep nulls.

- The planet signal is modulated against the bright radiation background. This is done using phase chopping. The combination of rotation, phase chopping, and averaging over time reduces the noise level by a factor of 100 to 10^{-7} of the stellar intensity.
- The technique of spectral fitting uses correlations between null fluctuations across the spectral band to reduce the instability noise. This yields a further factor of 10 in reduction of the noise level.

Thus, the combination of these four techniques yields the necessary performance. The current objective is to demonstrate the first three parts of this process; the stable nulling, the array (or planet) rotation and the phase chopping. At the time of writing, the PDT has demonstrated detection of a planet 2 million times fainter than the star using some simplified methods. The testbed is now being prepared for faint planet detection using the first three techniques. The suppression effect achieved using these techniques in which the nulled starlight at 10^{-5} is reduced to 10^{-7} will be representative of flight performance. Validation of the fourth technique, spectral fitting, will be left to a future plan.

Figure 4-23. The Formation Control Testbed (FCT). Shown here are the two robots of the FCT. Each robot carries cannisters of compressed air that allow them to float off a polished metal floor. The floor is flat to within 2 one-thousandths of an inch and spans a much larger area than shown here. The robots serve as the hardware interface and testing ground for flight software developed for space applications in formation flying. (Courtesy Caltech/JPL/NASA)

Guidance, Navigation, and Control

The Formation Control Testbed (FCT) was built to provide an end-to-end autonomous formation-flying system in a ground-based laboratory. The FCT provides an environment for system-level demonstration and validation of formation-control algorithms. The algorithms are validated using multiple floating test robots that emulate real spacecraft dynamics. The goal is to demonstrate algorithms for formation acquisition, formation

maneuvering, fault-tolerant operations, as well as collision-avoidance maneuvering. (See Lawson et al. 2008 and references therein.)

The FCT is comprised of two robots with flight-like hardware and dynamics, a precision flat floor for the robots to operate on, ceiling-mounted artificial stars for robot attitude sensing and navigation, and a "ground control" room for commanding the robots and receiving telemetry. The robots and part of the flat floor are shown in Figure 4-23. The layout of the FCT emulates the environment of a formation of telescopes that is restricted to maneuvering in the same plane in space, normal to the direction of the target star.

To be as flight-like as possible, each robot is equipped with a typical single-spacecraft attitude-control suite of reaction wheels, gyros, and a star tracker. Thrusters are also available for attitude control. Each robot has a lower translational platform and an upper attitude platform. The attitude platform is the "spacecraft" and is completely disconnected from the translational platform.

- The attitude platform/spacecraft houses the avionics, actuators, sensors, inter-robot and "ground"-to-robot wireless communication antennas, and spacecraft processors.
- The translational platform provides both translational and rotational degrees of freedom to the attitude platform via (i) linear air bearings (the black, circular pads at the base of each robot) that allow the entire robot to float freely on the flat floor, and (ii) a spherical air bearing at the top of the vertical stage (the black, vertical cylinders).

In 2007 the FCT demonstrated precision maneuvers using two robots, showing autonomous initialization, maneuvering, and operation in a collision-free manner. The key maneuver that was demonstrated was representative of TPF-I science observations. Repeated experiments with the robots demonstrated formation rotations through greater than 90° at ten times the flight rotation rate while maintaining a relative position control to 5 cm RMS. Although the achievable resolution in these experiments was limited by the noise environment of the laboratory, it was nonetheless demonstrated through modeling that in the relatively noise-free environment of space, the performance of these algorithms would exceed TPF-I flight requirements.

Propulsion Systems

Missions employing Precision Formation Flying (PFF) require propulsion capabilities that exhibit low plume contamination, high thrust precision, and high power and propellant efficiency. Ion thrusters typically deliver low-contamination plumes and high efficiency by using noble gas propellants, but conventional thrusters provide thrust levels over an order of magnitude greater than the sub-milli-Newton (mN) to mN levels needed for precision-controlled formation-flying space interferometer missions.

A miniature ion thruster, the Miniature Xenon Ion (MiXI) thruster developed at JPL, is a new option that meets mission needs. One particularly useful characteristic of the MiXI thruster is its incredibly large thrust range that provides smooth amplitude modulated thrust in the 0.1–3.0 mN in the amplitude modulated mode and 0.001–0.1 mN of thrust in pulse-width modulation (PWM) mode (patent-pending). With a minimum on-time of less than 1 ms, the MiXI thruster can provide impulse bits of less than 1 $\mu N \cdot s$ at low power levels. The PWM mode of the MiXI thruster is achieved by precision control of the thruster voltages.

4.3.4 Future Milestones

Probe-Scale Mission

Table 4-3 is a summary of the technical readiness levels (TRLs) of key technologies used in the probe-scale mission (FKSI). These levels are estimated using NASA standard terminology (Mankin 1995).

Many of the key technological hurdles for FKSI, as understood in the original studies performed in 2002–2003, have been solved by NASA flagship projects. In particular, the investments in *JWST* and TPF-I/Darwin technologies can be directly used in the FKSI system. As of early 2007, *JWST* passed all of its key technology milestones, including those for cryocoolers, precision cryogenic support structures, detectors, cryogenic mirrors, and sunshades. All of these technologies can be adapted to the FKSI mission with little effort.

Key technologies unique to the FKSI mission have also benefited from NASA's investments in the Keck Interferometer Nuller system (now in operation at the Keck Observatory) and the TPF-I testbeds at JPL, including the Planet Detection Testbed and the Achromatic Nuller Testbed. The broadband null depths from these testbeds are about an order of magnitude better than the requirements for the FKSI mission.

The optical fibers needed for wavefront cleanup have been fabricated and tested at room temperature as part of the TPF-I technology program. Currently two types of fibers have been tested in the laboratory and work sufficiently well for the FKSI mission: these are chalcogenide fibers fabricated at the Naval Research Laboratory (NRL) (Aggarwal & Sanghera 2002) that operate from the near- to mid-infrared, and silver halide fibers developed at Tel Aviv University that operate in the longer wavelength part of the mid-infrared (see Ksendzov et al. 2007 and references therein). A third type of fiber, a hollow glass waveguide fiber developed at Rutgers University (Harrington 2001) may also be of use. Further testing is planned, including cryogenic testing of all fibers.

Table 4-3. Technical Readiness Levels for Key Subsystem Components

Item	Description	TRL	Notes
1	Cryocoolers	6	Source: *JWST* T-NAR
2	Precision cryogenic structure (booms)	6	Source: *JWST* T-NAR
3	Detectors (near-infrared)	6	Source: *HST*, *JWST* Nircam T-NAR
4	Detectors (mid-infrared)	6	Source: *Spitzer* IRAC, *JWST* MIRI T-NAR
5	Cryogenic mirrors	6	Source: *JWST* T-NAR
6	Optical fiber for mid-infrared	4	Source: TPF-I
7	Sunshade	6	Source: *JWST* T-NAR
8	Nuller Instrument	4–5	Source: Keck Interferometer Nuller, TPF-I project, LBTI
9	Precision cryogenic delay line	6	Source: TNO

*Note: The requirement for the FKSI project is a null depth of 10^{-4} in a 10% bandwidth. Laboratory results with the TPF-I testbeds have exceeded this requirement by an order of magnitude (Lawson et al. 2008).

At the system level, a nuller instrument fabricated at JPL has been delivered to and is in use at the Keck Observatory. The FKSI nuller instrument is actually simpler than the Keck instrument, as the latter requires chopping out the background created by a warm telescope and sky (not needed by FKSI). Indeed the first data from the Keck Interferometer Nuller has

recently been published (Barry et al. 2008). The Bracewell Infrared Nulling Cryostat (BLINC, Hinz et al. 2000) is a cryogenic nuller in use on the MMT, which has achieved significant results in studies of accretion disks around Herbig Ae/Be stars.

Although the BLINC system is a vacuum cryogenic nuller subsystem, and in many respects is similar to what is required for the FKSI nulling instrument, a high-fidelity vacuum cryogenic nulling testbed that provides an environment with the expected space-like signal and thermal noise levels and that also includes representative disturbance forces, would be of great benefit to the FKSI mission itself, and could be used as a relatively low cost starting point for a much more complex cryogenic nulling testbed that is needed for the flagship TPF-I/Darwin missions, as discussed below. Such a cryogenic testbed would reduce cost and technical risk for both the Probe-class mission as well as the flagship mission.

Finally, FKSI requires a precision cryogenic delay line with a stroke of the order of a centimeter. Fortunately, commercial firms in Europe, under contract from ESA have developed such a prototype cryogenic delay line, which is at a high TRL level. This delay line has a precision of 1.3 nm and a stroke of 10 mm, which is more than adequate for a small interferometer. Also, two short-stroke cryogenic delay lines have been flown as part of two Michelson spectral interferometers, both of which were developed at the Goddard Space Flight Center. One was the FIRAS instrument on the COBE mission, which won a Nobel Prize in Physics for Drs. John Mather and George Smoot for cosmic microwave background research (see for example, Mather et al. 1994, Wright et al. 1994). A second has been flown successfully on the CASSINI mission, as part of the CIRS instrument (http://saturn.jpl.nasa.gov/spacecraft/inst-cassini-cirs-details.cfm).

In summary, we note the two areas for further technology development for a small infrared structurally-connected interferometer: (1) At the component level, cryogenic testing of the optical fibers for wavefront cleanup; and (2) at the system level, a vacuum cryogenic nulling testbed.

Single-Mode Filters Demonstrated in a Cryogenic Vacuum, 6–20 μm

The single-mode fibers used in the Adaptive Nuller are made of chalcogenide material and have been demonstrated to yield 25 dB or more rejection of higher-order spatial modes, thus meeting the flight requirements (Ksendzov et al. 2007). Because this material becomes opaque at wavelengths above 12 μm, other materials must be used in the 12–20 μm wavelength band. Silver halide single-mode fibers have been demonstrated to meet flight requirements at 10 μm, and should also work well at longer wavelengths (Ksendzov et al. 2008). Although this performance is sufficient for flight, it would be greatly advantageous to improve the throughput of these devices, to test them throughout the full wavelength range they are intended for, and to test them cryogenically. Spatial filter technology would then be at TRL 5. It would, furthermore, be advantageous to implement mid-infrared spatial filters and beam combiners using integrated optics, so as to reduce the risk associated with the complexity of the science instruments.

Cryogenic Adaptive Nulling

Adaptive nulling is straightforward to generalize over a full science band, and it should be demonstrated within a cryogenic vacuum, bringing the technology to TRL 5. This would necessitate the successful validation of cryogenic spatial filters (above) and the testing of a cryogenic deformable mirror.

Planet Detection System in a Cryogenic Vacuum

The final demonstration for the feasibility of a probe-scale mission would be to integrate all the necessary components in a vacuum cryogenic testbed. This would demonstrate the full system complexity and include flight-like servo systems and brass-boards of the components described previously.

Flagship Mission

The technology program for the Terrestrial Planet Finder Interferometer is now close to achieving all of its milestones in starlight suppression. The basic component technology for starlight suppression at mid-infrared wavelengths is now at TRL 4. TRL 5 requires testing in a relevant environment, which for TPF/Darwin would be a cryogenic vacuum near 40 K. Most research so far has been undertaken in air at room temperature. As will be discussed below, sufficient progress has now been made that the greatest advance in this area would be to proceed to brass-board designs of already successful components and subsystems, and to implement system-level cryogenic testing.

Ground-based demonstrations with the Formation Control Testbed (FCT) have shown that the Guidance, Navigation, and Control algorithms now exist to execute precision maneuvers with two telescopes (Scharf 2007; Scharf & Lawson 2008). Additional testing should be carried out to validate collision avoidance and fault tolerant algorithms, but the greatest advance would be to transition to space-based demonstrations in collaboration with our European colleagues.

Future technology demonstrations are discussed as follows.

Planet Detection with Chopping and Averaging

Further noise suppression is required in addition to starlight suppression. Nulling can reduce the glare of starlight to a level fainter than the warm glow of local zodical dust (surrounding our Sun) and exo-zodiacal dust (around the target star), but the planet itself may still be 100 times fainter. The technique for detecting and characterizing planets therefore relies on several other strategies.

The first step is to suppress the response to any thermal emission that is symmetrically distributed around the star. In principle this will remove the detected glow of local and exozodiacal dust. By rotating the array and averaging the response, the planet signal can be further enhanced. The beam combiner for TPF/Darwin therefore combines two pairs of beams to null the starlight, and the beam combining system modulates the response on the sky (keeping the star nulled) by chopping back and forth between these nulled pairs. This milestone has been detailed in the Whitepaper for the Planet Detection Testbed (Martin et al. 2008c).

Broadband Systematic Noise Suppression

An additional step is required to suppress the noise down below the typical brightness of an Earth-like planet. After nulling and chopping, the dominant source of noise is due to residual instabilities in the null depth, which generates a white-noise of similar intensity to the planet signal. This noise can be suppressed by appropriate choice of interferometer baselines and by filtering the measured data from a complete rotation of the array. We expect this milestone will be completed by the Planet Detection Testbed in 2009.

Additional technology progress beyond this milestone would depend on cryogenic testing of components and systems.

Planet Detection Demonstration in a Flight-like Environment

Laboratory work is well advanced to demonstrate the detection of planet light with the Planet Detection Testbed. Simulated planets two million times fainter than a star have been detected in early trials, and the work is ongoing. Although these tests represent the full complexity of beam combination, this research is being conducted at room-temperature in air, and the noise properties of the testbed are therefore unlike those that would be met in flight. Following the completion of this work, the next step would be to build a vacuum cryogenic beam combiner with flight-like servo systems, including the brass-board components described above.

Guidance, Navigation, and Control: Collision Avoidance, Fault Detection

Additional tests that could be carried out with the FCT include demonstrating new capabilities such as (1) reactive collision avoidance, (2) formation fault detection, and (3) autonomous reconfiguration and retargeting maneuvers. Also, using a real-time simulation environment would allow the demonstration of performance with full formation-flight complexity, with five interacting spacecraft showing synchronized rotations, autonomous reconfigurations, fault detection, and collision avoidance.

In-flight Testing of Formation Algorithms

National agencies in Europe are actively advancing the technology of formation flying, with flight missions starting in 2009–2014. The European Space Agency and national space agencies in Europe have a program of precursor missions to gain experience in formation flying. In 2009 the Swedish Space Agency will launch the Prisma mission. This is primarily a rendezvous and docking mission, but it will also test RF metrology designed for Darwin. In 2012 ESA plans to launch Proba-3, which will include optical metrology loops for sub-millimeter range control over a 30-m spacecraft separation. The French and Italian space agencies are planning to launch Simbol-X in 2015. Simbol-X is an X-ray science mission with separate detector and lens spacecraft with a 20-m spacecraft separation. Simbol-X should enter Phase B of development in early 2009.

Although two-spacecraft precision maneuvers were demonstrated in 2007, a major goal that remains is to demonstrate robust algorithms for three or more spacecraft, such as would be used by TPF-I (Lawson et al. 2008). The opportunity no doubt exists to leverage the expertise developed for TPF-I in collaboration with European colleagues. The greatest advance in maturing technology for formation flying would be to have a modest-scale technology mission devoted to verifying and validating guidance and control algorithms. Such in-flight testing would be made even more meaningful if it could include the interferometric combination of starlight from separated platforms.

A ground-based facility such as the FCT should continue to provide the means to test and improve real-time formation-flying algorithms as the technology matures, even while the technology is being proven in space.

4.4 Research & Analysis Goals

4.4.1 Ground-Based Interferometry

Ground-based interferometry serves critical roles in exoplanet studies. It provides a venue for development and demonstration of precision techniques including high-contrast imaging and nulling, it trains the next generation of instrumentalists, and it develops a community of scientists expert in their use. With the highest priority, nulling facilities should be refined and operated for the characterization of debris disks and exozodiacal light and the impact of these on direct detection missions.

Ground-based interferometry can also provide unique support to exoplanet studies. RV detections have been vetted for the possibility of stellar companions on highly inclined orbits (Baines et al. 2008a). Transit planets can be studied more precisely with direct measurement of the stellar diameters (Baines et al. 2008b). Keck and VLTI will soon offer precision narrow-angle astrometry, intermediate between *HST* and SIM, that will open new areas of exoplanet parameter space, and will improve the characterization of known exoplanet systems, contributing to construction of well-understood target lists for direct detection missions. Ground-based interferometers may soon be capable of direct detection and study of some of the very brightest exoplanets (Monnier et al. 2006).

We endorse the recommendations of the "Future Directions for Ground-based Optical Interferometry" Workshop (Akeson et al. 2007) and the ReSTAR committee report (Bailyn et al. 2008) to continuing vigorous refinement and exploitation of existing ground-based interferometric facilities (Keck, NPOI, CHARA, and MRO), widening of their accessibility for exoplanet programs, and continued development of interferometry technology and planning for a future advanced facility.

The nature of Antarctic plateau sites, intermediate between ground and space in potential, offers significant opportunities for exoplanet and exozodi studies by interferometry and coronagraphy (Kenyon et al. 2006; Coudé du Foresto et al. 2006). Balloon altitudes are also promising for high-contrast imaging (Traub & Chen 2007). Further evaluation of these opportunities should be encouraged and supported, with the expectation that they may be competitive for future implementation.

4.4.2 Theory Support

In order to achieve our most ambitious goals of relating exoplanet atmospheres composition to planet formation, system evolution, surface chemistry and biology, we will require sustained support of strong astrobiology and atmospheric chemistry programs.

4.4.3 Space-Based Interferometry

Space-based interferometry serves critical roles in exoplanet studies. It provides access to a spectral range that cannot be achieved from the ground, and it can characterize the detected planets in terms of atmospheric composition and effective temperature. Sensitive technology has already been proven for missions like *JWST*, SIM, and *Spitzer*, and within NASA's preliminary studies of TPF. With high priority, technology for nulling interferometers in space should be advanced to make the next generation spacecraft to detect and characterize the closest planets flight ready.

4.4.4 Agency Coordination and Programmatic Synergies

The very broad scientific and public interest in exoplanets, and the direct relevance to both NASA and NSF goals, makes it an ideal topic for coordination between the agencies, and we urge NASA and NSF staff to leverage this relationship to cover the full breadth of exoplanet science and technology.

4.4.5 International Cooperation, Collaboration, & Partnership

In past years (2002–2006) a NASA/ESA Letter of Agreement (LOA) has allowed the US and European communities to develop a joint TPF and Darwin mission concept based on a convergence of science requirements, design studies, and shared technology goals. The relationships forged between US and European collaborators should again be fostered over the next decade to further studies of small mission and flagship mission concepts. A new letter of agreement is necessary to renew these collaborations.

4.5 Contributors

Olivier Absil, Université de Grenoble, Joseph Fourier

Rachel Akeson, Caltech, NASA Exoplanet Science Institute

John Bally, University of Colorado

Richard K. Barry, NASA Goddard Space Flight Center

Charles Beichman, NASA Exoplanet Science Institute

Adrian Belu, Université de Nice Sophia Antipolis

Mathew Boyce, Helios Energy Partners

James Breckinridge, Caltech, Jet Propulsion Laboratory

Adam Burrows, Princeton University

Christine Chen, Space Telescope Science Institute

David Cole, Caltech, Jet Propulsion Laboratory

David Crisp, Jet Propulsion Laboratory

William C. Danchi, NASA Goddard Space Flight Center

Rolf Danner, Northrop Grumman Space Technology

Peter Deroo, Caltech, Jet Propulsion Laboratory

Vincent Coudé du Foresto, Observatoire de Paris

Denis Defrère, Université de Liège

Dennis Ebbets, Ball Aerospace and Technology Corporation

Paul Falkowski, Rutgers University

Robert Gappinger, Jet Propulsion Laboratory

Ismail D. Haugabook, Sr., Digital Technical Services
Charles Hanot, Caltech, Jet Propulsion Laboratory, Université de Liège
Phil Hinz, Steward Observatory, University of Arizona
Jan Hollis, NASA Goddard Space Flight Center
Sarah Hunyadi, Jet Propulsion Laboratory
David Hyland, Texas A&M University
Kenneth J. Johnston, U. S. Naval Observatory
Lisa Kaltenegger, Harvard Smithsonian Center for Astrophysics
James Kasting, Pennsylvania State University
Matt Kenworthy, Steward Obsevatory, University of Arizona
Alexander Ksendzov, Jet Propulsion Laboratory
Benjamin Lane, Draper Labs
Gregory Laughlin, UCO Lick
Peter Lawson, Caltech, Jet Propulsion Laboratory
Oliver Lay, Caltech, Jet Propulsion Laboratory
Réne Liseau, Stockholm University
Bruno Lopez, Observatoire de la Cote d'Azur
Rafael Millan-Gabet, Caltech, NASA Exoplanet Science Institute
Stefan Martin, Caltech, Jet Propulsion Laboratory
Dimitri Mawet, Caltech, Jet Propulsion Laboratory
Bertrand Mennesson, Caltech, Jet Propulsion Laboratory
John Monnier, University of Michigan
Naoshi Murakami, National Astronomical Observatory of Japan (NAOJ)
M. Charles Noecker, Ball Aerospace and Technology Corporation
Jun Nishikawa, National Astronomical Observatory of Japan (NAOJ)
Meyer Pesesen, Caltech, Jet Propulsion Laboratory
Robert Peters, Caltech, Jet Propulsion Laboratory
Alice Quillen, University of Rochester
Sam Ragland, W. M. Keck Observatory
Stephen Rinehart, NASA Goddard Space Flight Center
Huub Rottgering, University of Leiden
Daniel Scharf, Caltech, Jet Propulsion Laboratory
Eugene Serabyn, Caltech, Jet Propulsion Laboratory
Motohide Tamura, National Astronomical Observatory of Japan (NAOJ)

Mohammed Tehrani, The Aerospace Corporation

Wesley A. Traub, Caltech, Jet Propulsion Laboratory

Stephen Unwin, Caltech, Jet Propulsion Laboratory

David Wilner, Harvard-Smithsonian Center for Astrophysics

Julien Woillez, W. M. Keck Observatory

Neville Woolf, University of Arizona

Ming Zhao, University of Michigan

4.6 References

Aggarwal, I. D., & Sanghera, J. S. 2002, "Development and applications of chalcogenide glass optical fibers at NRL," J. Optoelectron. Adv. Matter, 4, 665–678

Akeson, R., Allen, R., Angel, R., et al. 2007, *Workshop on the Future Directions for Ground-based Optical Interferometry: Final Report*, National Optical Astronomy Observatory, Tucson, AZ, http://www.noao.edu/meetings/interferometry/Workshop-report.pdf

Angel, J. R. P., & Woolf, N. J. 1997, "An imaging nulling interferometer to study extrasolar planets," ApJ, 475, 373–379

Baines, E. K., McAlister, H. A., ten Brummelaar T. A., et al. 2008a, "The search for stellar companions to exoplanet host stars using the CHARA Array," ApJ, 682, 577–585

Baines, E. K., McAlister, H. A., ten Brummelaar T. A., et al. 2008b, "CHARA Array measurements of the angular diameters of exoplanet host stars," ApJ, 680, 728–733

Bailyn, C., Barnes, T., et al. 2008, *Renewing Small Telescopes for Astronomical Research*, ReSTAR Report, National Optical Astronomy Observatory, Tucson, AZ, http://www.noao.edu/system/restar/files/ReSTAR_final_14jan08.pdf

Barry, R. K., Danchi, W. C., et al. 2005, "The Fourier-Kelvin Stellar Interferometer (FKSI): a progress report and preliminary results from our nulling testbed," Proc. SPIE, 5905, 311–321

Barry, R. K., Danchi, W. C., et al. 2006, "The Fourier-Kelvin Stellar Interferometer: a low-complexity low-cost space mission for high-resolution astronomy and direct exoplanet detection," Proc. SPIE, 6265, 62651L

Barry, R. K., Danchi, W. C., Koresko, M. C., et al. 2008, "High-Resolution N-Band Observations of the Nova RS Ophiuchi with the Keck Interferometer Nuller," ApJ, 677, 1253–1267

Beichman, C. A., Woolf, N. J., & Lindensmith, C. A., eds. 1999, *The Terrestrial Planet Finder (TPF): a NASA Origins Program to Search for Habitable Planets*, JPL Publication 99-3, Jet Propulsion Laboratory, Pasadena, California

Beichman, C. A., Fridlund, M., Traub, W. A., Stapelfledt, K. R., Quirrenbach, A., & Seager, S. 2006, "Comparative planetology and the search for life beyond the Solar System," *Protostars and Planets V*, editors Riepurth, B., et al., University of Arizona Press, Tucson, AZ, 915–928

Booth, A. J., Martin, S. R., & Loya, F. 2008, "Exoplanet Exoploration Program Planet Detection Testbed: latest results of planet light detection in the presence of starlight," Proc. SPIE, 7013, 701320

Beaulieu, J.-P., Bennett, D. P., et al. 2006, "Discovery of a cool planet of 5.5 Earth masses through gravitational microlensing," Nature, 439, 437–440

Bracewell, R. N. 1978, "Detecting nonsolar planets by spinning infrared interferometer," Nature, 274, 780–781

Christensen, P. R. & Pearl, J. C. 1997, "Initial data from the Mars Global Surveyor thermal emission spectrometer experiment: Observations of the Earth," J. Geophys. Res., 102, 10875–10880

Cockell, C. S., Herbst, T., Léger, A., et al. 2009, "Darwin—A Mission to Detect, and Search for Life on, Extrasolar Planets," Astrobiology, in press, preprint, arXiv:0805.1873

Coudé du Foresto, V., Absil, O., Swain, M., Vakili, F., & Barillot, M. 2006, "ALADDIN: an optimized nulling ground-based demonstrator for DARWIN," Proc. SPIE, 6268, 626810

Crawford, S. L., Colavita, M. M., Garcia, J. I., et al. 2005, "Final laboratory integration and test of the Keck Interferometer nuller," Proc. SPIE, 5905, 59050U

Danchi, W. C., Deming, D., Kuchner, M., & Seager, S. 2003a, "Detection of Close-In Extrasolar Giant Planets with the Fourier-Kelvin Stellar Interferometer," ApJL, 597, L57

Danchi, W. C., Allen, R., Benford, R. J., et al. 2003b, "The Fourier-Kelvin Stellar Interferometer," in *Towards Other Earths: DARWIN/TPF and the Search for Extrasolar Terrestrial Planets*, Heidelberg, Germany, 22–25 April 2003 (ESA Publication SP-539, October 2003)

Danchi, W. C., Allen, Barry, R., Benford, R. J., et al. 2004, "The Fourier-Kelvin Stellar Interferometer: A Practical Interferometric Mission for Discovering and Investigating Extrasolar Giant Planets," Proc. SPIE, 5491, 236

Danchi, W. C., & Lopez, B., 2007, "The Fourier-Kelvin Stellar Interferometer (FKSI) — A practical infrared space interferometer on the path to the discovery and characterization of Earth-like planets around nearby stars," Comptes rendus - Physique (C.R. Physique), 8, 396–407

Defrère, D., Absil, O., Coudé du Foresto, V., Danchi, W. C., & den Hartog, R. 2008, "Nulling interferometry: performance comparison between space and ground-based sites for exozodiacal disc detection," A&A, 490, 435–445

Des Marais, D. J., Harwit, M. O., Jucks, K. W., Kasting, J. F., Lin, D. N. C., Lunine, J. I., Schneider, J., Seager, S., Traub, W. A., & Woolf, N. J. 2002, "Remote sensing of planetary properties and biosignatures of extrasolar terrestrial planets," Astrobiology, 2, 153–181

Forget, F., & Pierrehumbert, R. T. 1997, "Warming early Mars with carbon dioxide clouds that scatter infrared radiation," Science, 278, 1273–1276

Frey, B. J., Barry, R. K., Danchi, W. C., et al. 2006, "The Fourier-Kelvin Stellar Interferometer (FKSI) nulling testbed II: Closed-loop pathlength metrology and control subsystem," Proc. SPIE, 6265, 62651N

Fridlund, M. 2000, *DARWIN: The InfraRed Space Interferometer*, ESA-SCI (2000)12, 47 European Space Agency: Noordwijk, The Netherlands

Fridlund, C.V.M., Gondoin, P., Bavdaz, M. et al. 2008, "Feather-light touch all that's needed for Darwin's frictionless optics," in the ESA website; http://www.esa.int/esaCP/SEMD3J8J50F_index_0.html

Gappinger, R. O., Diaz, R. T., Ksendzov, A., Lawson, P. R., Lay, O. P., Liewer, K., Loya, F. M., Martin, S. R., Serabyn, E. & Wallace, J. K. 2009, "Experimental evaluation of achromatic phase shifters for mid-infrared starlight suppression," Appl. Opt., 48, 868-880

Gould, A., Udalski, A., An, D., et al. 2006, "Microlens OGLE-2005-BLG-169 implies that cool Neptune-like planets are common," ApJ, 644, L37–L40

Harrington, J. A. 2001, *Infrared Fiber Optics*, M. Bass, J. Enoch, E. Van Stryland, & W. Wolfe, eds., (McGraw-Hill, New York).

Hinz, P. M., Angel, J. R. P., et al. 2000, "BLINC: a testbed for nulling interferometry in the thermal infrared," Proc. SPIE, 4006, 349–353

Hinz, P. M., Heinze, A. N., et al. 2006, "Thermal infrared constraint to a planetary companion of Vega with the MMT adaptive optics system," ApJ, 653, 1486–1492

Hyde, T. T., Liu, K-C., Blaurock, C., Bolognese, J., et al. 2004, "Requirements Formulation and Dynamic Jitter Analysis for the Fourier-Kelvin Stellar Interferometer," Proc. SPIE, 5491, 553

Kaltenegger, L., Eiroa, C., Stankov, A., Fridlund, M. 2009, "The Darwin target star catalog," Astrophys. & Space Sci., in press

Kaltenegger, L., & Fridlund, M. 2005, "The Darwin mission: Search for extra-solar planets," Advances in Space Research, 36, 1114–1122

Kaltenegger, L., Traub, W. A., & Jucks, K. 2007, "Spectral evolution of an Earth-like planet," ApJ, 658, 598–616

Karlson, A. L., Wallner, O., Armengol, J. M. P., et al. 2004, "Three telescope nuller based on multibeam injection into single-mode waveguide," Proc. SPIE, 5491, 831–841

Kasting, J. F., Whitmire, D. P., & Reynolds, R. T. 1993, "Habitable zones around main sequence stars," Icarus, 101, 108–128

Kasting, J. F., & Catling, D. 2003, "Evolution of a habitable planet," ARA&A, 41, 429–463

Kenyon, S. L., Lawrence, J. S., et al. 2006, "Atmospheric scintillation at Dome C, Antarctica: Implications for photometry and astrometry," PASP, 118, 924–932

Ksendzov, A., Lay, O., Martin, S., Sanghera, J. S., Busse, L. E., Kim, W. H., Pureza, P. C., & Nguyen, V. Q. 2007, "Characterization of mid-infrared single mode fibers as modal filters," Appl. Opt., 46, 7957–7962

Ksendzov A., Lewi T., Lay, O. P., Martin, S. R., Gappinger, R. O., Lawson, P. R., Peters, R. D., Shalem, S., Tsun, A., & Katzir, A. 2008, "Modal filtering for midinfrared nulling interferometry using single mode silver halide fibers," Appl. Opt., 47, 5728–5735

Kurland, R. 2007, "JWST Sunshield Silicon-Coated Membrane Material: Summary-Level Report," JWST Technical Non-Advocate Review (T-NAR), January, 17 2007, Goddard Space Flight Center, Greenbelt, MD

Lafrenière, D., Jayawardhana, R., van Kerkwijk, M. H., "Direct imaging and spectroscopy of a planetary mass candidate companion to a young Solar analog," ApJL, 689, L153–L156, 2008

Lawson, P. R., Lay, O. P., Martin, S. R., Peters, R. D., Gappinger, R. O., Ksendzov, A., Scharf, D. P., Booth, A. J., Beichman, C. A., Serabyn, E., Johnston, K. J., & Danchi, W. C., 2008, "Terrestrial Planet Finder Interferometer: 2007–2008 progress and plans," Proc. SPIE, 7013, 7013N

Lawson, P. R., Lay, O. P., Martin, S. R., et al. 2007, "Terrestrial Planet Finder Interferometer: 2006–2007 progress and plans," Proc. SPIE, 6693, 669308

Lay, O. P. 2004, "Systematic errors in nulling interferometers," Appl. Opt., 43, 6100–6123

Lay, O. P. 2005, "Imaging properties of rotating nulling interferometers," Appl. Opt., 44, 5859–5871

Lay O. P. 2006, "Removing instability noise in nulling interferometers," Proc. SPIE, 6268, 62681A

Lay, O. P., Martin, S. R., & Hunyadi S. L. 2007, "Planet-finding performance of the TPF-I Emma architecture," Proc. SPIE, 6693, 66930A

Léger, A., Mariotti, J.-M., Mennesson, B., Ollivier, M., Puget, J. L., Rouan, D., & Schneider, J. 1996, "Could we search for primitive life on extrasolar planets in the near future?: The DARWIN Project," Icarus, 123, 249–255

Léger, A., Herbst, T., et al. 2007, "DARWIN mission proposal to ESA," 23 Jul 2007. arXiv:0707.3385v1 [astro-ph].

Lopez, B., S. Wolf, S. Lagarde, P. Abraham, et al. 2006, "MATISSE: perspective of imaging in the mid-infrared at the VLTI," Proc. SPIE, 6268, 31

Lovelock, J. E., 1975, "Thermodynamics and the recognition of alien biospheres [and discussion]," Proc. R. Soc. Lond. B 189, 167–181

Lunine, J. I. 2001, "The occurrence of Jovian planets and the habitability of planetary systems," PNAS, 98, 809–814

Mankins, J. C., 1995, "Technology Readiness Levels," NASA Advanced Concepts Office, Office of Space Access and Technology, National Aeronautics and Space Administration, Washington, DC, http://www.hq.nasa.gov/office/codeq/trl/trl.pdf.

Martin, S. R., Serabyn, E., Hardy, G. J. 2003, "Deep nulling of laser light in a rotational shearing interferometer," Proc. SPIE, 4838, 656–667

Martin, S. R. 2005, "The flight instrument design for the Terrestrial Planet Finder Interferometer," Proc. SPIE, 5905, 21–35

Martin, S. R. 2006, "Progress in four-beam nulling: results from the Terrestrial Planet Finder Planet Detection Testbed," in 2006 IEEE Aerospace Conference, Big Sky, Montana

Martin, S. R., Szwaykowski, P., Loya, F., Liewer, F. 2006, "Progress in testing exo-planet signal extraction on the TPF-I Planet detection Testbed," Proc. SPIE, 6268, 626818

Martin, S. R., Scharf, D., Wirz, R. et al. 2007, "TPF-Emma: concept study of a planet finding space interferometer," Proc. SPIE, 6693, 669309

Martin, S. R., Scharf, D. P., Wirz, R., et al. 2008a, "Design Study for a Planet-Finding Space Interferometer," IEEE Aerospace Conf, Big Sky, Mt, USA

Martin, S. R., Serabyn, E., Liewer, K. 2008b, "The development and applications of a ground-based fiber nulling coronagraph," Proc. SPIE, 7013, 70131Y

Martin, S. R., Booth, A. J., Lay, O. P., & Lawson, P. R. 2008c, *Exoplanet Interferometry Technology Milestone #4 Whitepaper: Planet Detection Demonstration*, Jet Propulsion Laboratory Document D-47627, http://planetquest.jpl.nasa.gov/TPF-I/TPF-I_M4_Whitepaper_Final.pdf

Mather, J. C., Cheng, E. S., Cottingham, D. A., et al. 1994, "Measurement of the Cosmic Microwave Background Spectrum by the COBE FIRAS Instrument," ApJ, 420, 439–444

Mennesson, B., Haguenauer, P., Serabyn, E., & Liewer, K. 2006, "Deep broad-band infrared nulling using a single-mode fiber beam combiner and baseline rotation," Proc. SPIE, 6268, 626830

Monnier, J. D., Pedretti, E., et al. 2006, "Michigan Infrared Combiner (MIRC): commissioning results at the CHARA Array," Proc. SPIE, 6268, 62681P

National Research Council, 2001, *Astronomy and Astrophysics in the New Millennium*, http://www.nap.edu/openbook.php?isbn=0309070317

Ollivier, M. 1999, *Contribution à la Recherche d'Exoplanète: Coronagraphie Interférentielle pour la Mission Darwin*, Ph.D. thesis, University Paris XI

Owen, T. 1980, "The search for early forms of life in other planetary systems," in *Strategies for Search for Life in the Universe*, editors Papagiannis, M. D., Springer: Dordrecht, The Netherlands, p. 177

Peters, R. D., Lay, O. P., Jeganathan, M. 2008, "Broadband phase and intensity compensation with a deformable mirror for an interferometric nuller," Appl. Opt., 47, 3920–3926

Ressler, M. 2007, "Mid-Infrared Detectors," JWST Technical Non-Advocate Review (T-NAR), 30–31 January 2007, Goddard Space Flight Center, Greenbelt, MD

Samuele, R., Wallace, J. K., Schmidtlin, E., Shao, M., Levine, B. M., Fregoso, S. 2007, "Experimental progress and results of a visible nulling coronagraph," 2007 IEEE Aerospace Conference, Big Sky Montana, paper 1333

Scharf, D. P. 2007, *TPF-I Milestone #2 Whitepaper: Formation Control Performance Demonstration*, Jet Propulsion Laboratory, Pasadena, CA, http://planetquest.jpl.nasa.gov/TPF-I/TPFI_M2_WhitePaper_Final.pdf

Scharf, D. P., Lawson, P. R. 2008, *TPF-I Milestone #2 Report: Formation Control Performance Demonstration*, Jet Propulsion Laboratory, Pasadena, CA, JPL Publication 08-11, http://planetquest.jpl.nasa.gov/TPF-I/TPFI_M2_ReportV3.pdf

Scharf, D. P., Hadaegh, F. Y., Keim, J. A., & Lawson, P. R. 2008, "Ground demonstration of synchronized formation rotations for precision, multi-spacecraft interferometers," in Proc. *3rd International Symposium on Formation Flying, Missions and Technologies*, Fletcher, K., ed., ESA SP-654 (CDROM)

Seager, S., Richardson, L. J., Hansen, B. M. S., et al. 2005, "On the Dayside Thermal Emission of Hot Jupiters," ApJ, 632, 1122–1131

Segura, A., Krelove, K., Kasting, J. F., Sommerlatt, D., Meadows V., Crisp D., Cohen, M., & Mlawer, E. 2003, "Ozone concentrations and ultraviolet fluxes on Earth-like planets around other stars," Astrobiology, 3, 689–708

Segura, A., Kasting, J. F., Meadows, V., Cohen, M., Scalo, J., Crisp, D., Butler, R. A. H., & Tinetti, G. 2005, "Biosignatures from Earth-like planets around M Dwarfs," Astrobiology, 5, 706–725

Selsis, F. 2000, "Physics of Planets I: Darwin and the Atmospheres of Terrestrial Planets," *Darwin and Astronomy: The Infrared Space Interferometer*, ESA SP 451, European Space Agency, Noordwijk, The Netherlands, pp. 133–140

Selsis, F., Despois, D., & Parisot, J.-P. 2002, "Signature of life on exoplanets: Can Darwin produce false positive detections?" A&A, 388, 985–1003

Selsis, F., Kasting, J. F., Levrard, B., et al. 2007, "Habitable planets around the star Gliese 581?," A&A, 476, 1373–1387

Serabyn, E., Wallace, J. K., Hardy, G. J., Schmidtlin, E. G. H., Nguyen, H. T. 1999, "Deep nulling of visible laser light," Appl. Opt., 38, 7128–7132

Serabyn, E., Booth, A.J., Colavita, M.M, et al. 2004, "The Keck interferometer nuller: system architecture and laboratory performance," Proc. SPIE, 5491, 806–815

Traub, W. A., & Chen, P., "Planetscope precursor experiment," BAAS 211, 30.06 (2007).

Turnbull, M. C., Traub, W. A., Jucks, K. W., Woolf, N. J., Meyer, M. R., Gorlova, N., Skrutskie, M. F., & Wilson, J. C. 2006, "Spectrum of a habitable world: Earthshine in the near-infrared," ApJ, 644, 551–559

Turnbull, M. C., *The Search for Habitable Worlds: From the Terrestrial Planet Finder to SETI*, Ph.D. Thesis, University of Arizona, ISBN 0496037129

Wallace, K., Hardy, G., Serabyn, E. 2000, "Deep and stable interferometric nulling of broadband light with implications for observing planets around nearby stars," Nature 406, 700–702

Wallner, O., Armengol, J. M. P., & Karlson, A. L. 2004, "Multiaxial single-mode beam combiner," Proc. SPIE, 5491, 798–805

Wright, E. L., Mather, J. C., Fixsen, D. J., et al. 1994, "Interpretation of the COBE FIRAS CMBR Spectrum," ApJ, 420, 450–456